
# The Role of Pathological Mechanical Environment on Cardiomyocyte Function in Hypoplastic Left Heart Syndrome

**An honors thesis for the Department of Biomedical Engineering**

**Ray Wang**

**Advisor: Dr. Lauren D. Black III, Department of Biomedical Engineering**
**Mentors: Corin Williams, Kelly Sullivan and Kathy Ye**

**Table of Contents**

**Abstract**

Left heart hypoplastic syndrome (HLHS) is a congenital heart defect (CHD) consisting of malformations in the left heart causing significantly inhibited blood flow. Currently surgical procedures have allowed infants to survive this condition into adulthood; however, these surgeries do not restore normal structure or function to the heart. Although improved treatment is desired, lack of understanding to the cause of HLHS hinders development. Therefore, this study aimed to isolate the role of the real-time stretched mechanical environment on healthy and diseased cardiac cell development. The mechanical environments were generated by a custom-built cell stretching device and tests were performed to validate output. To study HLHS, a nitrofen-induced disease rat model was created and fetal hearts were isolated at various time points. These hearts were characterized by qRT-PCR and Western blotting to determine phenotypic traits of the disease model. Cardiac cells from these fetal hearts were then cultured while stretched by our device and analyzed by the same methods. Based on our analysis, we determined relatively good correlation between the designated parameters and the actual output of the device in terms of membrane stretch and frequency; however improvements could be made. Additionally, CHD fetal hearts were determined to have shifts in gene expression and protein content related to decrease in contractile function and maturity. Furthermore, culture of cells under mechanical stimulation demonstrated increased gene expression conveying improved functionality and maturation. However, current incompatibility of myocyte adhesion to the silicone culture membrane under mechanical stretch limited our analysis for specific effects of different types of mechanical stimulation. Based on these results, application of mechanical cues characteristic of normal myocardial stretch to healthy or diseased cardiomyocytes could be utilized to promote gene expression for improved myocyte function.

**Acknowledgements**

I would like to thank my graduate student mentors, Kelly Sullivan and Kathy Ye, for their help with cardiac cell isolation, cell culture and quantification of the results by qRT-PCR and Western blot. I would also like to thank Corin Williams, a post doctorate in the Black Lab, for her mentorship and aid throughout the project. They were all incredibly helpful in planning, optimizing and executing this project. Furthermore, I would like to express my appreciation to my thesis and general lab advisor, Professor Black, head of the BME department, Professor Kaplan, my academic advisor Professor Omenetto and additional member of my thesis committee, Prof. Cronin. Thanks to their guidance and support, I was given the opportunity to undertake and contribute to this project along with receiving assistance from the Tufts University's Biomedical Engineering Department and funding from the American Heart Association.

## Index of Tables and Figures

# 1. Introduction

## 1.1 Significance

Congenital heart defects (CHDs) are the leading cause of death due to a birth defect in the United States with an estimated 36,000 affected infants per year (AHA Statistical Update, 2011). Among CHDs, hypoplastic left heart syndrome (HLHS) accounts for around 25% of all CHD mortalities (Loffredo 2000). Up until the 1980s, diagnosis of HLHS was lethal with 95% of infants dying in the first month after birth (Fruitman 2000). Since then, a series of palliative surgical treatments have been developed that has allowed many individuals to survive this condition. These surgeries correct for deformed heart structure by directing blood flow to prevent mixing of oxygenated and deoxygenated blood. However, surgical treatment of HLHS is the most expensive neonatal hospital procedure with an average cost of $199,597 (AHA Statistical Update, 2011). Moreover, the patient still requires lifelong monitoring, immunosuppressants and restriction of physical activity, which greatly decreases their quality of life (Latal 2009).

Although studies of HLHS have made many breakthroughs in determining genetic links for some cases of HLHS development, the majority of HLHS cases are believed to be due to non-genetic factors. Unfortunately, the significant factors causing heart malformations that lead to HLHS during prenatal stages are not well understood (Jenkins 2007). Based on *in vivo* models and case studies, a dominant hypothesis is HLHS development results from a cellular response to abnormal mechanical cues from their native environment due to altered blood flow in the left side of the heart (Correia-Pinto 2003). Unfortunately, current studies with *in vivo* models lack the capability to control significant biological factors possibly influencing HLHS which makes their specific roles difficult to discern. This lack of control hinders our

understanding of HLHS and development of better treatments to replace current surgical methods that do not restore normal function to the heart. Therefore, the goal of this project is to determine the specific role of mechanical cues from abnormal myocardial stretch in the left ventricle. Isolation of this role is significant because establishing the influence of individual factors critical to HLHS development can shift and improve treatment methods to target these factors.

### 1.2 Specific Aims and Hypotheses

The overall goal of this study was to improve our understanding of how mechanical stimulus mimicking the regular dynamic stretch of the myocardial membrane environment along with variations to that environment influence phenotypic traits of healthy and HLHS rat cardiomyoctes.

In reach our goal, we focused on the following specific aims:

**The first specific aim was to assess the output of our custom-built cell stretcher to validate generation of the designated mechanical environment.** For our study, we utilized a custom-built cell stretcher to stretch cell culture membranes to model the real-time regular stretching of the left ventricle tissue heart. By varying parameters such as controlled frequency and amplitude variability based on a set distribution, we generated various models of the myocardial environment for cardiac cells. Considering our device is custom-made, it was important that we validated the characteristics of the generated environments based on the designated parameters before performing cell studies in Specific Aim 3; otherwise it would be difficult to correlate characteristics of the mechanical environment to changes in myocardiocyte phenotype.

**The second specific aim was to determine the initial phenotypic traits of cardiac cells isolated from healthy and CHD rat models to assess whether mechanical environments influenced cultured cardiac cells towards a normal or pathological state**. A CHD rat model was created by providing a dose of nitrofen dissolved in olive oil at 10 days gestation to pregnant Sprague-Dowley rats to induce congenital diaphragmatic hernia and subsequent HLHS development in the fetuses. These rats were sacrificed at E15, F18 and F21 of gestation and hearts from the fetuses were isolated. As a control, another set of Sprague-Dowley rats provided olive oil alone at 10 days gestation was similarly sacrificed and fetal hearts were isolated at matching days of gestation. These hearts were separated into three groups of CHD+, CHD- and control based on the observation of a congenital diaphragmatic hernia development when treated with nitrofen. RNA and protein samples were extracted from a collection of the heart samples. Phenotypic traits were determined by RNA and protein quantification using qRT-PCR and Western blotting respectively for biomarkers of cardiomyocyte function and maturation.

**The third specific aim was to determine the effects of dynamic mechanical stimulation and variations to the stimulus on phenotypic development of healthy and HLHS cardiac cell.** Cardiac cells were extracted from the fetal hearts isolated from our CHD model characterized in Specific Aim 2. Based on *in vivo* studies; we hypothesized that the phenotype of fetal cardiomyocytes was dependent on the biomechanical cues received from the regularly stretched environment. To study this hypothesis, we generated healthy and HLHS-based diseased rat groups and cultured these isolated cardiomyocytes in the mechanical environments generated in Specific Aim 1. We further hypothesized that environments generated in Specific Aim 1 modeling the healthy heart would induce normal phenotypic

development while a diseased model environment would induce diseased phenotypic development. For clinical relevance, we were interested in whether cardiomyocytes from diseased groups cultured in the healthy model environment would induce healthy phenotypic characteristics. Phenotypic traits were assayed by the same methods and biomarkers related to cardiomyocyte function and maturation in Specific Aim 2.

### 1.3 Long Term Goals

The long term goal of our research is to improve our understanding of how extracellular signals influence cardiomyocte development and proper heart formation to develop novel methods to treat CHDs. With improved understanding of how the *in vivo* cell environment influences cardiac cell development, we hope to contribute to the development of novel methods of treatment that improve survival and quality of life for afflicted infants. Understanding the isolated role of specific factors can aid development of methods that target or utilize these factors for diagnosis, intervention and therapy. Furthermore, this work can contribute to our understanding of how varying mechanical cues drive general cell development towards healthy and diseased phenotypes along with observation of how restoration of healthy cues could influence the diseased condition.

## 2. Background

### 2.1 Clinical Symptoms of Hypoplastic Left Heart Syndrome

Symptoms of hypoplastic left heart syndrome (HLHS) involve severe malformations to the left side of the heart which greatly hinders the heart's capability to sustain normal blood flow. These malformations include underdevelopment of the aorta, left ventricle and mitral

valve connecting the left atria to the left ventricle. Due to these characteristics, the left ventricle is usually closed off and a defect opening between the left and right atria allows blood to return into circulation. The atria connection allows mixing of oxygenated and deoxygenated blood within the heart. (Goldberg 2003). Due to these problems, the heart cannot efficiently pump blood which usually leads to death within a week unless surgical procedures are performed. Illustrations of a healthy and HLHS heart along with block diagrams summarizing blood flow in each case is displayed in Figure 1.

A few days following birth, an infant afflicted with hypoplastic left heart syndrome (HLHS) initially may seem outwardly healthy, despite the malformations of the left heart. The apparently normal phenotype is due to the right ventricle initially sustaining blood flow circulation by pumping blood to both the pulmonary and systemic circulation through the *patent ductus arteriosus* which connects the right ventricle to the aorta during neonatal stages. Within several days after birth, the *patent ductus arterosus* usually constricts and prevents the right ventricle from pumping blood to the systemic circulation, thus requiring neonatal treatment (Jalali 2011). Ultimately, underdevelopment and malformation of these critical left heart structures hinders the heart's ability to supply adequate blood flow to sustain the body's needs.

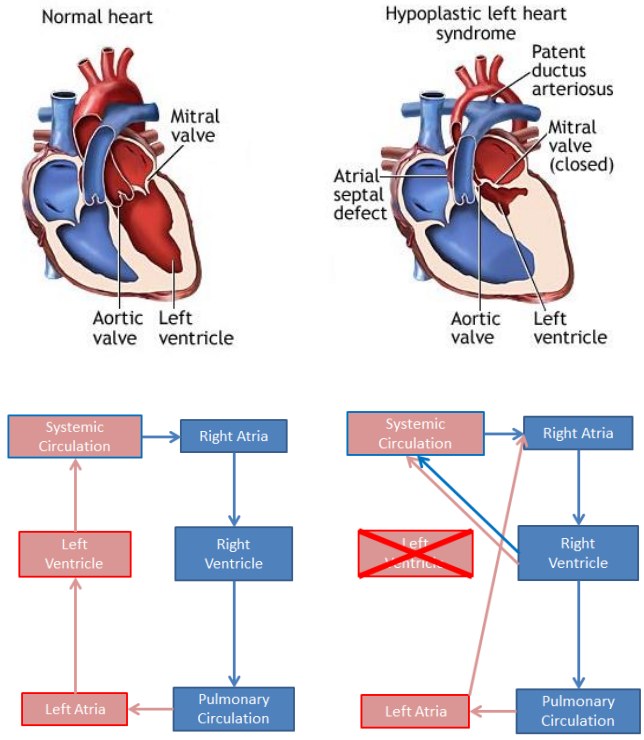


Figure 1: (Left) Image of a normal functioning heart where the left ventricle pumps blood to the systemic circulation. A summary of normal blood flow circulation is displayed in the block diagram below.
(Right) Image of a heart with hypoplastic left heart syndrome displaying an underdeveloped left ventricle, aorta and malformation such as the *atrial septal defect* and the *patent ductus arteriosus* that allows the right ventricle to pump blood to the systemic circulation. A summary of the altered blood flow circulation is displayed in the block diagram below (A.D.A.M. Medical Encyclopedia 2011).

## 2.2 Current Standard Methods of Treatment for Hypoplastic Left Heart Syndrome

The standard treatment for HLHS is performing a series of surgical procedures to prevent improper mixing of oxygenated and deoxygenated blood along with making the right ventricle dominant for pulmonary and systemic blood flow. HLHS is initially diagnosed by methods to examine impaired blood flow in the fetal heart such as echocardiogram or Doppler ultrasound (Ludman 1990). Shortly after birth, a Norwood procedure is performed connecting the main pulmonary artery to the aorta along with cutting off the connection to the lungs (Norwood 1980). To restore flow to the lungs, a shunt connection from either the aorta or right ventricle to the pulmonary artery is made, temporarily providing a controlled source of pulmonary circulation

(Sano 2003). After a period of 4 to 6 months, the shunt is removed and a Glenn operation connects the superior vena cava to the pulmonary artery to direct deoxygenated blood from the upper body straight to lungs (Kawashima 1984). Finally after 18 to 36 months, a Fontan operation connects the inferior vena cava to the pulmonary artery to direct deoxygenated blood from the lower body straight to the lungs (Fontan 1971, Kreutzer 1973). Overall, the right ventricle solely pumps oxygenated blood through the systemic circulation with deoxygenated blood passively flowing to the lungs.

Alternatively, a heart transplant can replace the malformed myocardium and restore healthy blood flow; however, these individuals require lifelong immunosuppressants to prevent immune rejection and there is a significant shortage of readily available hearts for transplant (Jalali 2011). Thus, further studies are needed to develop better treatments for HLHS patients that can help restore normal function to the heart.

## 2.3 Important Proteins related to Proper Myocyte Function and Maturation in Healthy and Diseased Development

### 2.3.1 Contractile Proteins

The heart is composed of muscle cells or cardiomyocytes whose growth and development during prenatal development are critical for proper heart function to pump blood through the systemic and pulmonary circulation. Studies of phenotypic differences between healthy and diseased tissue in *in vivo* models have generally been related to decreases in cardiomyocyte function and maturation based on shifts in protein and mRNA content (Correia-Pinto 2003). Protein groups of interest that are extensively studied are myocyte contractile, gap junction, channel and transcription factor proteins.

In mammalian cells, α and β isoforms of Myosin Heavy Chain (MYH) have been identified. These proteins are critical for the actual contractile mechanism by grabbing and pulling onto actin filaments (Jacot 2010). MYH-β has lower contractile function, but higher ratio of force to energy consumption ratio. In the ventricles, the β form predominates during early developmental stages in all mammalian species. In certain species such as rodents, MYH content shifts to α and becomes predominantly α by adulthood (Lompre 1984). In contrast, humans continue to maintain high β content with only 10% in the α isoform (Miyata 2000). However even though the content is minor, RNA and protein content are generally found to be severely decreased in humans during chronic heart failure (Nakao 1997). Additionally, large adjustments from α to β isoforms have been observed in mouse hearts undergoing heart failure possibly illustrating an adaptive response for improved energy conservation that eventually leads to overcompensation and decreased heart function (Harada 1999, Krenz 2004).

Troponin T (TnnT) and I (TnnI) proteins are critical for allowing myosin to bind to actin filaments. These proteins function by binding to the actin filament and inhibiting myosin binding respectively based on $Ca^{2+}$ binding (Hunkeler 1991). In addition, a common assay for injury to the heart is determination of released troponin proteins into the bloodstream (Tanindi 2011). These proteins are generally present in myocytes; however, specific isoforms are present in cardiac myocytes. Cardiac specific TNNI3 mRNA expression has been found to increase in fetal hearts during maturation along with a decrease general slow skeletal TNNI1 expression (Hunkeler 1991). Thus, proper expression and increases in cardiac specific isoforms are markers of both myocyte contractile function and maturation.

Finally, α-actinin is a major component of the sarcomere Z-disk allowing for anchoring and cross-linking of actin filaments along with roles in initiating signal pathways based on

mechanical load (Frank 2006). Due to its importance in proper sarcomere structure and function, mutations and shifts in expression of α-actinin have been linked to development of several cardiovascular diseases such as hypertrophic cardiomyopathy and HLHS (Chiu 2010, Gambetta 2008).

### 2.3.2 Gap Junction Signaling Proteins

Gap junction signaling proteins such as N-Cadherin and Connexin 43 (Cx43) are critical to proper myocyte connectivity and coordinated contraction amongst a population of myocytes. N-cadherin and Cx43 are cell surface proteins involved in cell-cell signaling for proper coordinated contraction and development (Vink 2004, Soler 1994). Studies inhibiting N-cadherin by antibody binding have demonstrated restricted contraction of individual and groups of myocytes (Soler 1994). Similarly extensive remodeling of the Cx43 is observed in diseased conditions and these alterations are related to improper contraction and arrhythmias (Vink 2004, Fontes 2012).

### 2.3.3 Channel Proteins

For myocyte contraction, proper $Ca^{2+}$ accumulation and flux mediated by channel proteins are required. Sacroendoplasmic reticulum calcium transport ATPase (SERCA) is an ion pump that drives $Ca^{2+}$ accumulation from the cytoplasm into the sarcoplasmic reticulum (Periasamy 2007). Release of $Ca^{2+}$ from the sacroendoplasmic reticulum is coordinated by ryanodine receptors (RyR) through a positive feedback mechanism for removing inhibition of TnnI (Kushnir 2010). Alterations in expression and activity of these proteins are related to

abnormal contractile and relaxation dysfunction in heart failure and other cardiac diseases (Periasamy 2007, Yano 2005).

### 2.3.4 Cardiac Transcription Factors

Finally, early cardiac transcription factors, GATA4, GATA6 and Nkx2.5 are critical for initial differentiation of cardiac cells and development of proper cardiac function. Therefore, inhibition of these proteins limits proper cardiomyocyte development and expression of these markers at later stages might indicate that a cardiac cell population is still immature (Sedmera 2002). Studies of nitrofen-induced CHD rat models have indicated decreased gene expression of GATA4 and GATA6 at early embryonic stages (Takayasu 2008). Therefore, we are interested in assaying these various proteins to determine phenotypic traits related to development of the CHD condition.

## 2.4 Evidence of the Influence of Mechanical Cues on Congenital Heart Disease Development

Although the cause of HLHS is not well understood, various studies have suggested an association between altered blood flow and HLHS development. Altered blood flow causes cardiac cells to experience abnormal biomechanical and biophysical cues. Support for this hypothesis stems from Doppler ultrasound imaging of a human fetus afflicted with aortic valve atresia, which often leads to development of HLHS. These ultrasound images conveyed a decreased strain and strain rate of left ventricle in the developing heart (Larsen 2006). Additional evidence of abnormal mechanical cues comes from associated HLHS development in congenital diaphragmatic hernia where the left heart is compressed from displaced organs.

Furthermore, cases of recovery from mild HLHS after surgical repair of congenital diaphragmatic hernia emphasize the role of mechanical cues and the possibility of restoring a healthy phenotype with intervention (Vogel M 2010). Thus, more research is necessary to better characterize how alterations to mechanical cues influence cardiomyocyte proliferation, maturation and function.

## 3. Material and Methods

### 3.1 Generation and Analysis of Dynamically Stretcher Mechanical Environment

#### 3.1.1 Custom-Built Cell Stretcher Device

Cell stretcher devices were designed to stretch the flexible silicone membrane of BioFlex® Culture Plates (Flexcell, McKeesport, PA) loaded onto the device. Underneath the culture plate was a set of six plungers for each well that contacted the membrane. Upward movement of the plungers into the underside of the membrane caused stretch. Movement of the plungers was induced by supplying power to a magnetic linear actuator and delivered to the plunger system by a lever connection. The magnetic linear actuator consisted of a solenoid surrounding a rod with single large ring-shaped neodymium super magnet. When a voltage was applied to the solenoid, an electromagnetic field was created which repels the magnets on the rod and caused the rod to move downward. The lever system was designed at a 3:1 ratio around the fulcrum so that the resultant force on the plunger was three times the incident force supplied from the linear actuator according to Archimedes Lever Principle.

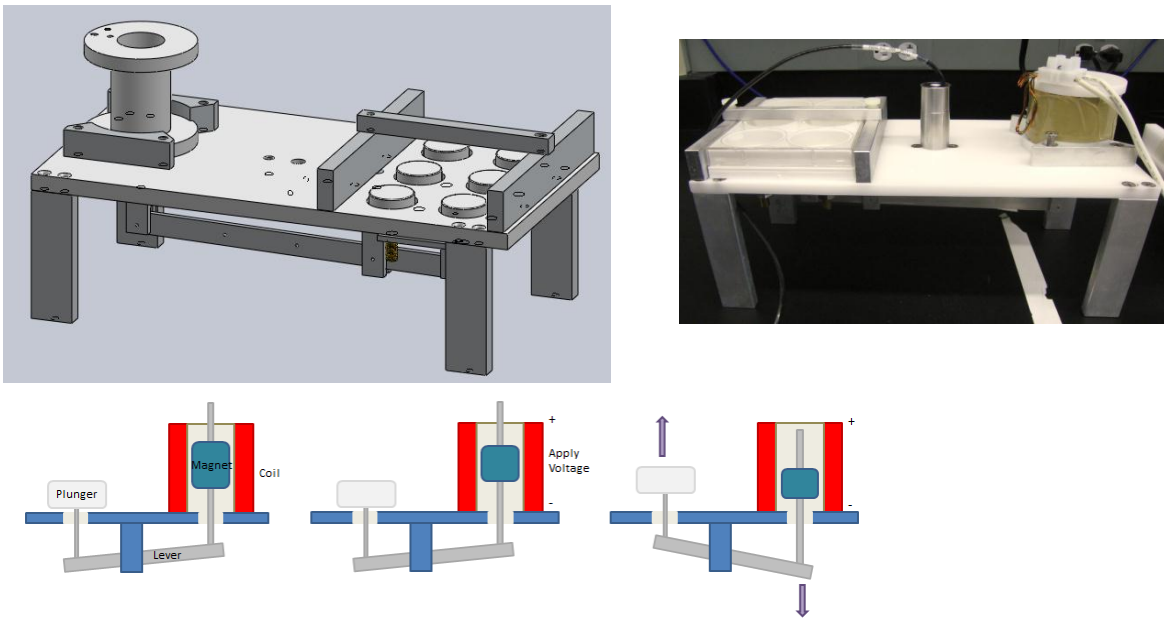


Fig. 2: (Left) Images of the 3D CAD model (Solidworks, Waltham, MA) of custom cell stretcher and (Right) the resulting device created through the Tufts Department of Biomedical Engineering machine shop. (Bottom) Illustration demonstrates how applying a voltage to the coil causes movement of the plunger.

### 3.1.2 Electronics to Power the Magnetic Linear Actuator of the Custom-built Cell Stretcher

An amplified pulse-width modulated (PWM) voltage signal was used to power the magnetic linear actuator through a metal-oxide-semiconductor field-effect transistor (MOSFET). A pulse train was generated for PWM by the counter outputs of National Instruments (NI) CompactDAQ 1-Slot USB Chassis (National Instruments, Austin, TX) with control of the duty cycle based on commands from a LabVIEW VI (National Instruments) control system.

### 3.1.3 Controller System to Generate Desired Mechanical Environments

Utilizing the capabilities of the custom-built cell stretcher device, an automatic control system was created to generate the desired mechanical environments. Specific mechanical environments were created based on a designating waveform, frequency and percent stretch. A proportional-integral-derivative (PID) feedback loop was used to calibrate the output of the

device to match the designated waveform shape and percent stretch. Feedback from the device was received from an LVDT which measured the movement of the plungers. Following calibration, mechanical environments with variability of frequency and amplitude based on a set distribution value and distribution type (constant, Gaussian and random) were generated.

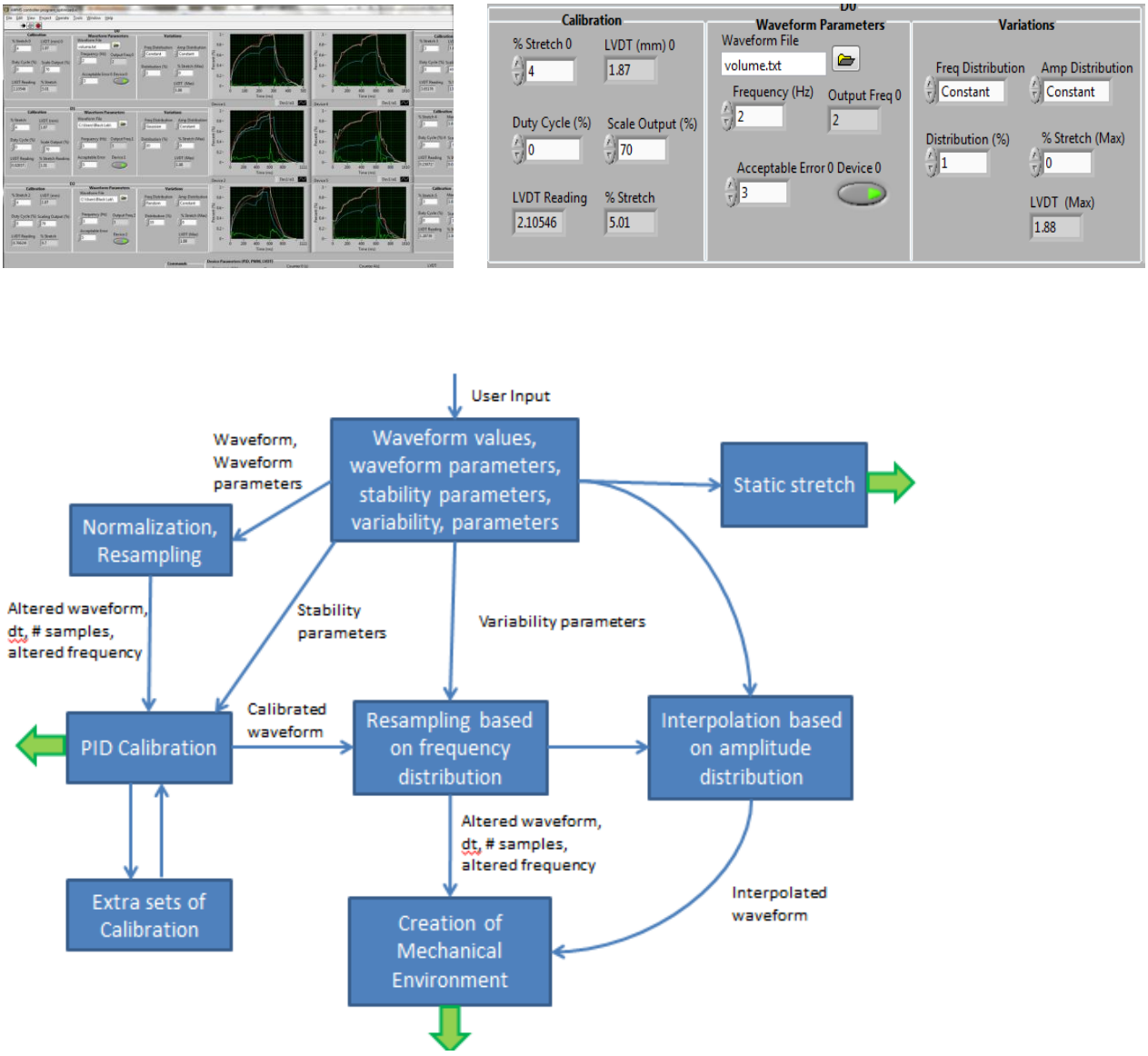


Fig. 3: Image of the user interface, user input panel and overview of the program process flow. User input demonstrates the input parameter requirements of percent stretch, frequency and waveform shape for outputting a waveform. Additional parameters of scaling factor, acceptable error and variability settings allow for creation of accurate and specific mechanical environments.

### 3.1.4 Calculation of Percent Stretch by Plunger Displacement and Image Analysis

The deformation of the membrane was modeled as a conical frustum based on the known dimensions of the well plate, plunger cap dimensions and known displacement of the plunger into the membrane. The theoretical percent stretch was calculated by the change in surface area due to the displacement of the plunger based on the following equations and conical frustum model,

$$\%\ Stretch = \frac{Final\ Surface\ Area - Initial\ Surface\ Area}{Initial\ Surface\ Area} * 100\%$$

$$SA_{conical\ frustum} = \pi(R_1 + R_2)\sqrt{(R_1 - R_2)^2 + h^2} + \pi {R_2}^2$$

$$SA_{circle} = \pi {R_1}^2$$

$$\%\ Stretch = \frac{\pi(R_1+R_2)\sqrt{(R_1-R_2)^2+h^2}+\pi {R_2}^2-\pi {R_1}^2}{\pi {R_1}^2} * 100\%$$

where $R_1$ was the radius of the well-plate (17 mm), R2 was the radius of the plunger cap (12.7 mm) and h was the displacement. This model assumed uniform stretch, low friction between the membrane-plunger interface and change in surface area only due to the displacement of the plunger into the membrane. This model was utilized by the controller system to determine the theoretical percent stretch based on the LVDT movement.

To determine percent stretch based on the membrane stretch; dots on the membrane surface were drawn to mark an area of interest. Video imaging of the membrane while being stretched was taken under different stretched conditions. Images were extracted and analyzed by ImageJ (NIH, Bethesda, MD) to calculate the % stretch.

### 3.1.5 Fast Fourier Transform for Analysis of Frequency and Distribution

LVDT readings were recorded over a long period of time and conversion of the recorded signal into the frequency domain was performed by built-in fast Fourier transform in MATLAB

(MathWorks, Natick MA). The transformed signal was plotted comparing amplitude versus frequency to observe frequency distributions.

### 3.2 Cell Line Creation, Isolation and Culture

#### 3.2.1 Nitrofen-Induced HLHS Disease Model Creation

To generate our HLHS-based disease model, pregnant Sprague Dawley® rats at 10 days gestation were placed under short isoflurane anesthesia and received a single 100 mg dose nitrofen (WAKO Chemical, Osaka, Japan) dissolved in olive oil by a gastric tube. As a control, normal rats were given a dose of olive oil without nitrofen. Cesarean section was performed by graduate student, Kelly Sullivan, and postdoc, Corin Williams, at 15, 18 and 21 days gestation during embryonic stages (E15) and fetal stages (F18, F21). The isolated fetuses were examined for presence of congenital diaphragmatic hernia and dissected under surgical stereoscope (Figure 1). Hearts were separated in groups of CHD-positive, nitrofen treated with an observed hernia (CHD+), CHD-negative, nitrofen-treated without an observed hernia (CHD-) and control groups.

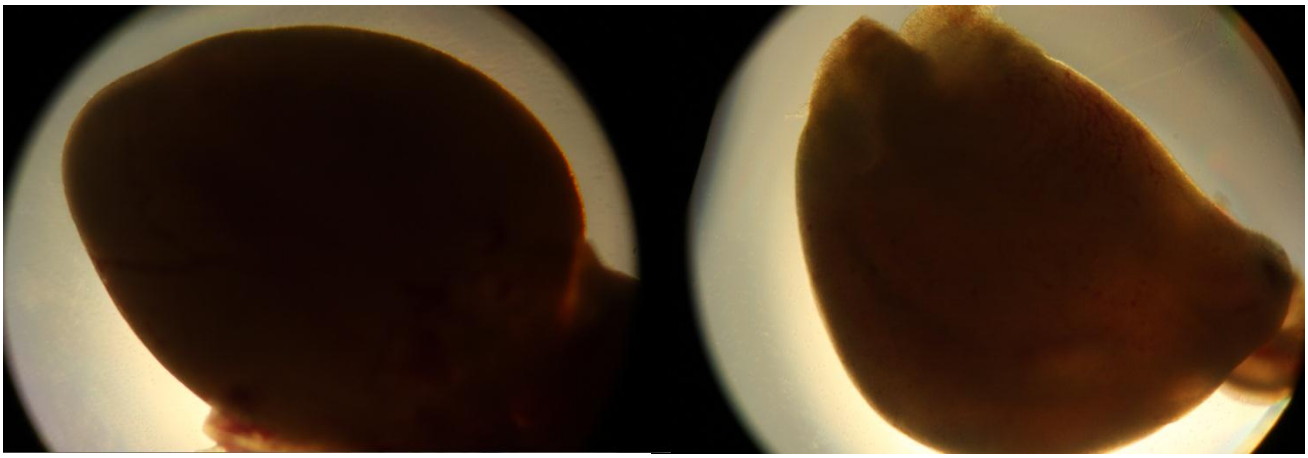

Figure 4: (Left) Image of healthy control heart isolated from fetus at F21.
(Right) Image of the nitrofen-induced diseased heart isolated from fetus at F21.

### 3.2.2 Cell Isolation

Cells were isolated from fetal hearts by repeated digested by adding 7 mL of warmed $37^0$ PBS solution containing 3.96 mg/mL glucose, 1% Penicillin Streptomycin (PS) and 300 U/mL collagenase type 2 (Worthington, Lakewood, NJ) incubated for 7 minutes at $37^0$C. Cell solution was filtered by 0.7 µm Sterile Cell Strainer (Fisher Scientific, Hampton, NH) and collagenase was inactivated by adding 10 mL of Stop Solution consisting of 5% fetal bovine solution (FBS) and 1% PS in Dulbecco's Modified Eagle Medium (DMEM) (Gibco, Grand Island, NY). Cells were pelleted by centrifugation at 500g for 5 minutes at $4^0$C and suspended in 4 mL of Myocyte Culture Media containing 10% horse serum (Sigma-Aldrich, St. Louis, Missouri), 2% FBS and 1% PS solution in DMEM. Cells were loaded into a hemocytometer and counted under a light microscope.

### 3.2.3 Cell Culture

Isolated cardiac cells from healthy and diseased models were seeded at ~900,000 cells/well on pre-coated Pronectin BioFlex Culture Plates® and incubated for three days in static conditions to allow time to adhere before loading onto the cell stretcher. Cells were mechanically stimulated for two days under designated conditions described previously. The underside of the flexible membrane was coated with silicone lubricant (Loctite, Düsseldorf, Germany) to minimize friction between the plunger and the membrane. The cardiac cells were fed by Myocyte Culture Media. Media was kept at 4°C and warmed to 37°C when fed to plated cells. Media was changed every two days.

### 3.2.4 Cell Collection for Protein and RNA Quantification

Following culture under mechanical stimulus, cells were removed from the silicone membrane by incubation in 0.05% trypsin (Gibco, Grand Island, NY) for two minutes and manual tapping of the culture plate. Trypsin was deactivated by quenching with FBS (50µL/well). Cells were pelleted by centrifugation at 500g for 5 minutes at 4°C and supernatant solution was aspirated from the pellet. Pellet was washed with PBS and pelleting processes was repeated.

## 3.3 RNA Extraction and Quantification

### 3.3.1 Cell Lysis for RNA Isolation and Purification by Silica Columns

Sample cell culture suspensions were lysed and isolated using RNeasy® Mini Kit (Qiagen Sciences, Germantown, MD). Cells were lysed by resuspension of pellet in 350 µL of provided Buffer RLT with 10 µL of added β-mercaptoethanol and genomic DNA was pelleted by centrifugation at max side. Supernatant was collected and 350 µL of 70% ethanol solution was added. Solution was transferred into a 2 mL silica column and centrifuged through at 8,000g for 15 seconds. 350 µL of Buffer RW1, 10 µL of DNase 1 treatment in 70 µL Buffer RDD for 15 minutes, 350 µL Buffer RW1, 500 µL Buffer RPE was added to the column and centrifuged through to wash and treat the sample. Column was dried by centrifugation at max speed and eluted into a collection tube by addition of 50 µL of nuclease-free water (Fischer Scientific, Hampton, NH) centrifuged through at 8,000g for 1 min.

### 3.3.2 Cell Lysis for RNA Isolation and Purification by TRIzol

Cells were lysed by resuspension of cell pellet in 900 µL of TRIzol Reagent (Ambion, Austin, TX) and incubation for 5 minutes at room temperature. Solution was mixed with 200 µL chloroform, vortexed for 15 seconds and rotated on the rotisserie for 3 minutes at room temperature. Aqueous and organic phases of the solution were separated by centrifugation at 12,000g for 15 minutes at $4^0$C. Aqueous phase was transferred into a separate tube and the organic phase was saved for protein extraction. Aqueous phase was mixed with 500 µL of isopropanol and incubated on a rotisserie for 1 hour at $-20^0$C to precipitate RNA. Precipitated RNA was pelleted by centrifugation at 12,000g for 15 minutes at $4^0$C and removal of supernatant. Pelleted RNA was washed in 1 mL of 75% ethanol, vortexed and centrifuged down again at 12,000g for 15 minutes at $4^0$C. Supernatant was removed and pellet was air dried for 10 minutes in a fume hood. RNA pellet was resuspended in 50 µL of nuclease-free water.

RNA was treated for residual contaminating DNA by DNA-free™ (Ambion). Treatment consisted of RNA sample mixed with 1 µL of rDNase I (2 U/µL) and one-tenth the total volume of 10X DNase I Buffer diluted in nuclease-free water. Solution mixture was incubated for 30 minutes at $37^0$C. rDNase I was inactivated by addition of DNase Inactivation Reagent and mixed for 2 minutes. Reagent was pelleted by centrifugation at 10,000g for 2 minutes and supernatant was collected.

### 3.3.3 RNA Purification and Quantification

Concentration of treated RNA was determined with Nanodrop 2000 Spectrophotometer (Thermo Scientific, Waltham, MA) and purity was assessed by the ratio of the 260/280 absorbance readings with a value close to 2.0 considered pure RNA.

### 3.3.3 cDNA Synthesis

cDNA was made using High Capacity cDNA Reverse Transcription Kit (Applied Biosystems, Foster City, CA). Up to 2 µg of RNA sample was reverse transcribed in 2 µL of 10X RT Buffer, 0.8 µL 25X dNTP Mix (100 mM), 2 µL of 10X RT Random Primers and 1 µL of MultiScribe$^{TM}$ Reverse Transcriptase (50 U/µL), and diluted with nuclease-free water to a final volume of 20 µL for each sample. Thermal cycling was performed with PTC-100 Programmable Thermal Controller (MJ Research Inc, Waltham, MA) with incubation parameters of 10 min at 25$^0$C, 120 min at 37$^0$C and 5min at 85$^0$C.

### 3.3.4 qRT-PCR (Taqman)

15 ng of cDNA was loaded into each well of a MicroAmp® Optical 96-well Reaction plate with 10 µL of 2X TaqMan® Gene Expression Master Mix and 1 µL of 20X TaqMan® Gene Expression Assay for the specific gene of interest (Applied Biosystems, Foster City, CA) diluted in nuclease-free water to a final volume of 20 µL. Samples were probed for gene expression related to contractile function (MYH6, MYH7, TNNT2, TNNI3, ACTN2, ATPA2), gap junction signaling (GJA1, CDH2) and markers of cardiac lineage (GATA4, GATA6, NKX2-5). Expression of these genes was normalized to GAPDH. qRT-PCR was performed with Mx3000P QPCR System (Agilent Technologies, Lexington, MA) with incubation parameters of

2 min at 50$^0$C, 10 min at 95$^0$C and 40-50 cycles of 15 seconds at 95$^0$C followed by 1 min of 60$^0$C.

### 3.3.5 Gene Expression Analysis

Ct values were determined by software provided with Mx3000P QPCR System and differences in mRNA expression was calculated by $2^{-\Delta\Delta ct}$ based on validation tests performed by Applied Biosystems.

## 3.4 Protein Extraction and Quantification

### 3.4.1 Cell Lysis for Protein Isolation

Cell pellet was resuspended in 100 µL of lysis buffer (50% 2X NP40, 2.5% 40X sodium deoxycholate, 1% 100X sodium orthovanadate, 0.1% 1000X aprotinin, 0.1% 1000X pepstatin, 0.1% leupeptin in deionized water) and sonicated by sonication needle for 20s on ice. Solution was then vortexed and then put on a rotisserie for 15 minutes at 4ºC.

### 3.4.2 Cell Lysis for Protien Isolation Following RNA Isolation through TRIzol

Separated organic phase from RNA isolation by TRIzol was mixed with 300 µL of 100%, incubated for 3 minutes at room temperature on a rotisserie and DNA pellet was centrifuged down at 5000g for 5 minutes at 4$^0$C. Supernatant was transferred into a separate tube and mixed with as much isopropanol as possible and incubated for 10 minutes at room temperature to precipitate protein. Protein was pelleted by centrifugation at 12,000g for 10 minutes at 4$^0$C and removal of supernatant. Pellet was washed 3 times in 2 mL of 0.3 M guanidine hydrochloride in 95% ethanol and once in 100% ethanol for 20 minutes on a rotisserie. Solution was pelleted off

and pellet was air dried in fume hood for 20 minutes. Protein pellet was resuspended in 0.5% SDS solution and heating for 10 minutes at $35^0$C.

### 3.4.3 BCA Assay for Total Protein Quantification

Total protein sample concentration was determined through Pierce® BCA Protein Assay Kit (Thermo Scientific, Rockford, IL). Samples were diluted 5 times and 10 µL triplicates of sample were pipetted into a 96 well plate. 200 µL of BCA working reagent consisting of Pierce® BCA Protein Assay Reagent A and B at a 1:20 ratio was added to each well and mixed thoroughly on an orbital. The plate was incubated for 30 minutes at 37ºC and absorbance was measured on a microplate reader at 560 nm. The absorbance was compared to a standard curve of bovine serum albumin (BSA) in lysis buffer to determine protein concentration.

### 3.4.4 Gel Electrophoresis and Western Blot Transfer to PVDF Paper

Based on the BCA protein assay, 10-15 µg of protein sample diluted in deionized water was mixed with sample buffer and 2M DTT at a 12:3:1 ratio. with a rainbow marker. Sample mixtures were vortexed, placed on a heat block for 5 minutes at 100ºC and quickly spun down. Samples were loaded into the 10 or 15 wells of a pre-made 4-15% Mini-PROTEAN® TGX™ Gels (Bio-Rad, Hercules, CA) with a mixture of Full Range Rainbow™ Recombinant Protein Molecular Weight Marker (GE Healthcare, Pittsburgh, PA) and Spectra™ Multicolor High Range Protein Ladder (Thermo Scientific). Gel were run in running buffer (3.03 g tris base, 1.44 g glycine and 1 g SDS in 1L of deionized water) at a constant 60 mA using Mini-PROTEAN® Tetra cell (Bio-Rad, Hercules, CA) till bands ran to the bottom of the gel. Then, protein was transferred to methanol activated PVDF membrane, (Immobilon® - P Transfer Membrane,

Millipore, Billerica, MA) in transfer buffer (3.03 g tris base, 1.44 g glycine, 200mg SDS, 20% methanol in 1 L deionized water). Transfer was run at a constant 90 mA overnight followed by 15 minutes at 150 mA, 15 minutes at 250 mA and 10 minutes at 350 mA. PVDF membrane was then dried under vacuum and reactivated for 2 minutes in 100% methanol.

### 3.4.5 Antibody Staining for Proteins of Interest

Membranes were blocked with 5% milk in Tris Buffered Saline at pH 7.6 mixed with 0.5% Tween-20 (TBST) for 1 hour at room temperature and probed with primary antibodies in 5% milk in TBST for 1 hour at room temperature. Membranes were washed 3 x 5 minutes with TBST and reacted with secondary antibody in 5% milk in TBST for 1 hour at room temperature. The blots were probed by primary antibodies for contractile proteins (MYH-α, MYH-β, TnnT, TnnI, α-actinin, SERCA), gap junction signaling proteins (Cx43, N-cadherin) and markers of cardiac lineage (GATA4, GATA6, NKX2-5) (Santa Cruz Biotechnology, Santa Cruz, CA) at dilutions of 1/400 primary and 1/1000 Horse Radish Peroxidase (HRP)-conjugated secondary antibodies for the respective primary animal (Invitrogen, Grand Island, NY). Proper transfer was evaluated by staining the gel with Imperial$^{TM}$ Protein Stain and the PVDF membrane staining with Pierce® Reversible Protein Stain Kit (Thermo Scientific, Rockford, IL). Membranes were exposed to chemiluminescence developed in G:Box using GeneSys software (Syngene, Pegasus Court, MD) after the application of ECL. All antibodies of interest were normalized to β-actin expression or calsequestrin expression. Western blots were quantified using ImageJ analysis (NIH).

# 4. Results

## 4.1 Evaluation of the Custom-Built Cell Stretchers Capability to Create a Designated Mechanical Environment

### 4.1.1 Generation of Mechanical Environment Mimicking the Real-time Dynamic Stretching of the Left Ventricle

To create a mechanical mimic of the myocardial membrane environment, designation of percent stretch, waveform and frequency parameters were needed. Percent stretch and frequency were restricted to 2% and 1 Hz to minimize harsh conditions on the cells that would cause loss of cell adhesion. Additionally, the dynamic stretch of the left ventricle was mimicked by stretch based on the left ventricular volumetric loading waveform. The waveform shape was created by three quadrants with vertical and horizontal composition of the waveform taken from an available textbook (Hall & Guyton 2011).

### 4.1.2 Evaluation of Theoretical Model for Membrane Percent Stretch

To assess for characteristics of the membrane stretch, video imaging of the membrane was taken and analyzed. Four points were drawn on a membrane from 25 to 150 mm equidistant from the center of the plunger in increments of 25 mms to mark off areas of interest. Video imaging was taken of the membrane gradually stretched by increasing duty cycle output increasing by 10% increments. Images at each incrementally stretched state were extracted and used for analysis. Marked regions of interest were extracted by image cropping and analyzed by ImageJ. Calculated percent stretches were corrected for displacement towards the camera by normalizing to the area of the plunger cap. These values were also compared with the theoretical percent stretch determined with our conical frustum model to assess its accuracy.

Experimental set-up consisted of loading the marked plate on a six plunger and four plunger systems for additional confirmation of observed behavior. The actual percent stretches determined by video imaging were found to be relatively uniform over the surface of the plunger as indicated by the small deviation around averaged values of the percent stretch 25 to 125 mm from the plunger center (Figure 5). Distribution of the percent stretch indicated maximum stretch occurred around 50 mm from the center with stretch gradually decreasing both towards and away from the center. Additionally, the relationship between plunger movement and percent stretch was observed to be relatively linear with $R^2$ values of 0.9758 and 0.9897 for the six and four plunger system respectively. Markings at 150 mm for the six plunger system were off the plunger-membrane interface and were determined to relatively stationary indicating lack of stretch in that area. Due to increased slant and shadow from the higher displacement in the four plunger system, marking at 125 and 150 mm were distorted and could not be properly extracted for analysis.

Comparison of the determined results with our theoretical model demonstrated relatively good correlation although actual results were generally higher expect towards the end of the theoretical curve. Comparison of the actual percent stretch distribution demonstrated higher determined stretch values from 25 to 75 mm and lower stretch values from 100 to 125 mm compared to the theoretical stretch. Additionally compared to the exponential shape of the theoretical model, percent stretch to plunger movement was demonstrated to be linear relationship especially at higher percent stretches. Thus although our current model allowed for a relatively good estimate of percent stretch, improvements to our model could be made to correct for these observed differences.

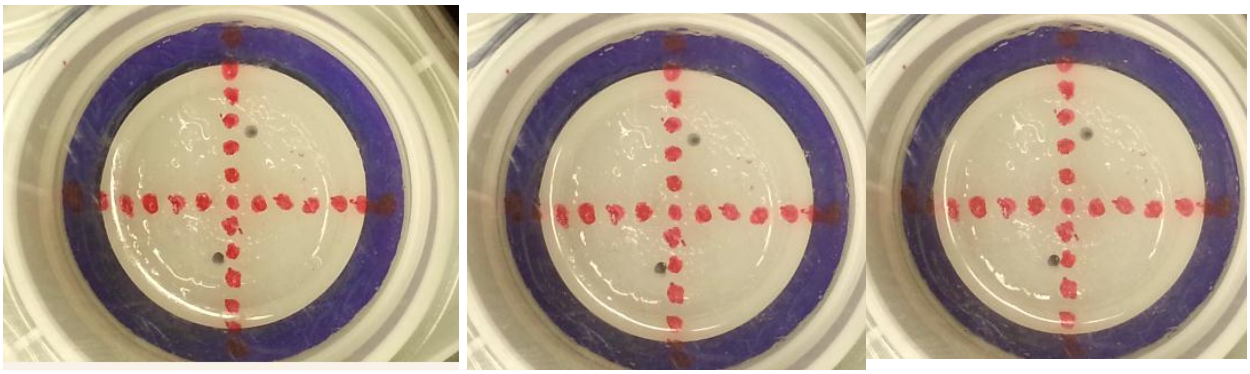

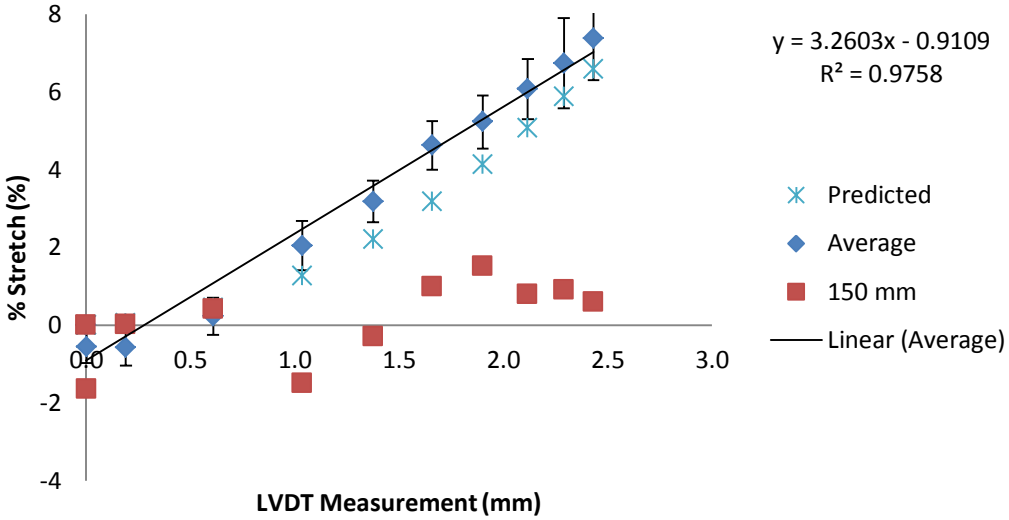
Video Analyzed Change in Percent Stretch to Plunger Movement: 6 Plunger System
% Stretch (%)
8
6
4
2
0
-2
-4
0.0
0.5
1.0
1.5
2.0
2.5
3.0
LVDT Measurement (mm)
y = 3.2603x - 0.9109
R² = 0.9758
Predicted
Average
150 mm
Linear (Average)

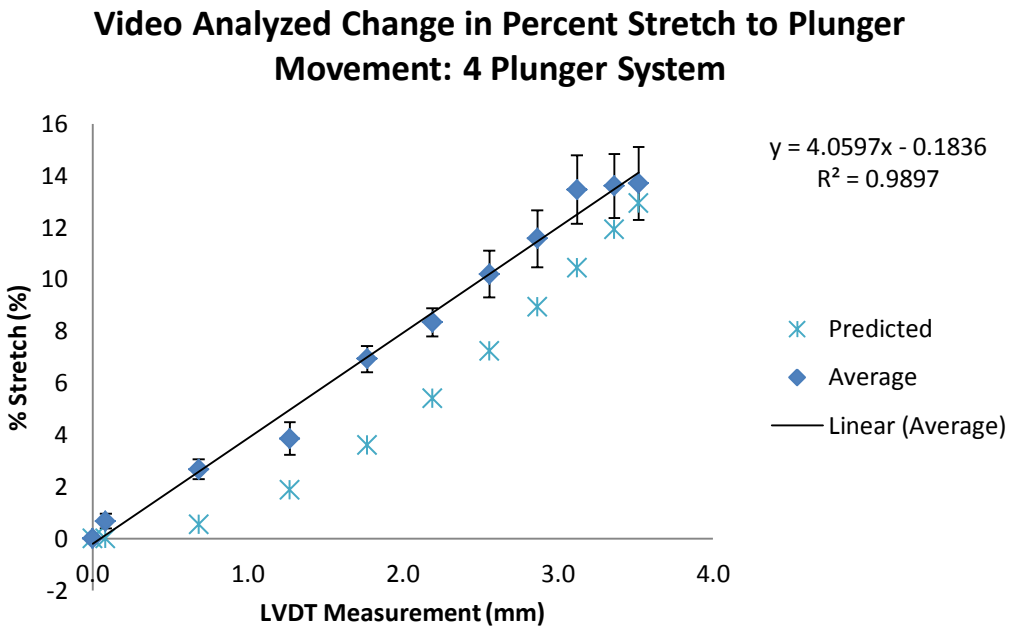


Figure 5: (Top) Images of the membrane while being stretched when supplying a PWM-voltage at 0, 50 and 100% duty cycle for the six plunger system.
(Middle) Plots of relationship between LVDT measurements on plunger movement to determined percent stretch based on change in marked areas of interest for six plunger system.
(Bottom) Plots of relationship between LVDT measurements on plunger movement to determined percent stretch based on change in marked areas of interest for four plunger system.

### 4.1.2 Evaluation of Waveform Generation

Generation of the designated waveform mimicking the volumetric loading waveform of the left ventricular to mimic the respective mechanical environment was evaluated by successful generation by PID calibration under experimental conditions. Six cell stretcher devices were simultaneously run at 1 Hz and 1% acceptable error. The PID equation was set to 0.1 for all PID parameters and calibration from a low output to 2.5% stretch was performed at a rate of 1 Hz. Plots of the LVDT measurement displayed expected calibration every second and the calibrated waveform displayed good fidelity with the ideal waveform indicating generation of the mechanical environment was successful under the experimental conditions. Due to sample

limitation, only four devices were used for cell culture experiments, thus our system was more than capable of creating our designated mechanical environment.

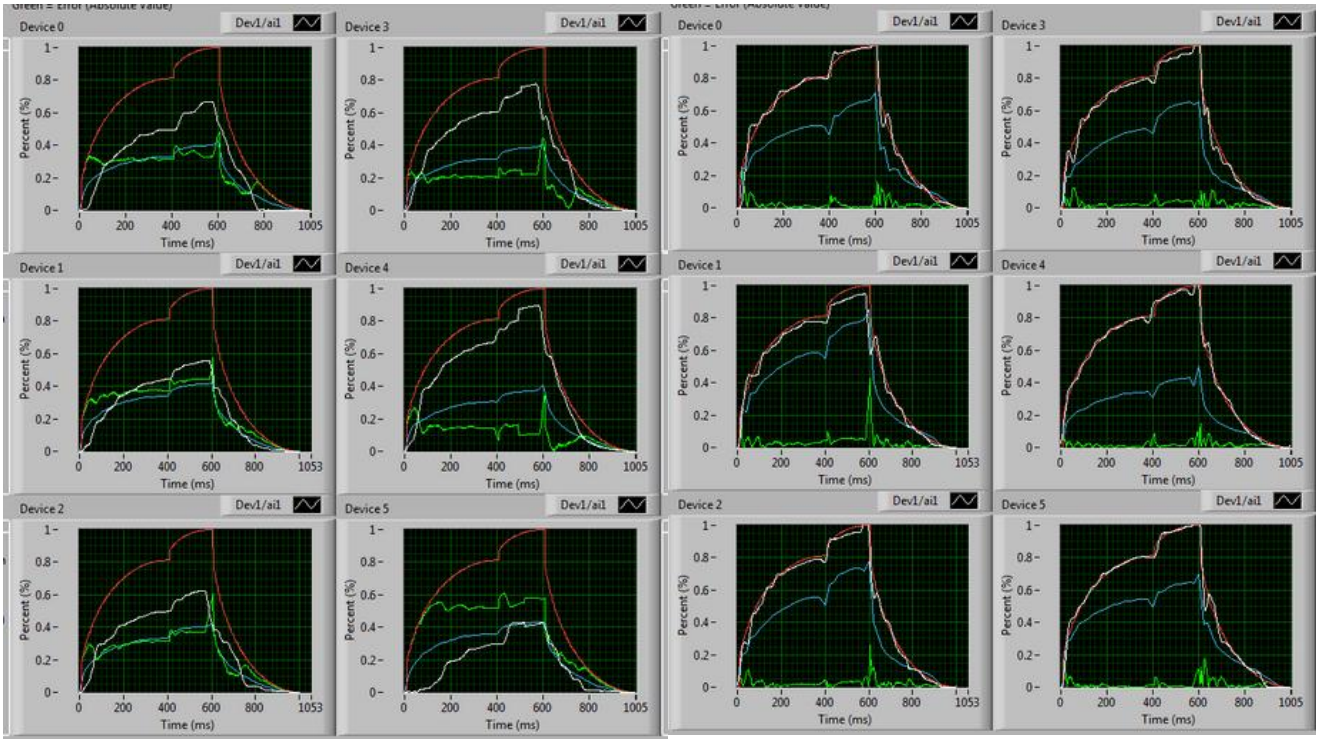


Figure 7: Plots displaying the ideal waveform in red, LVDT measurement in white, output in blue and error between the ideal and the LVDT measured in green. Four graphs for the four devices running at a 2.5% stretch, frequency of 1 Hz and a 1% acceptable error. Initial measurement (left) shows a large difference between the actual and ideal waveform generated. Plots after significant calibration had been completed (right) and simple output generation indicated that the average error between the ideal and actual output was at or below 1%.

### 4.1.3 Validation of Frequency

Considering that we wanted to assess the effects of changes in frequency and frequency distribution, it was important that significant lag to the system does not occur especially with multiple devices which would lead to an unassigned frequency distribution. To determine if significant lag occurred while the system was running multiple devices, LVDT readings were recorded and a fast Fourier Transform (FFT) of the data containing 50,000 waveforms was performed with MATLAB's built-in FFT functions. By the observing the distribution of frequencies from the transformed signal, we could assess whether significant unwanted

distribution occurred. LVDT readings recorded over a 6 hour period while running six devices simultaneously at 1 Hz were recorded and transformed into the frequency domain. A plot of the transformed signal running at 1 Hz displayed a sharp peak at 1 Hz with amplitude slightly over 0.8 with around a 0.2% distribution. Transformed plot for the device running at 2 Hz displayed a sharp peak slightly past 0.7 with around a 0.5% distribution. Additionally, we could also assess correct output of a set distribution by the same method. LVDT readings were recorded while devices were set to output either a Gaussian or random distribution. These results demonstrated a distributed output with minor peaks near the 0.9 and 1.1 Hz along with a sharp peak at 1 Hz due to initial calibration. Both plots did show a slight shift from the center at 1 Hz, however, these shifts were less than 1% and possibly due to the limited sample size of 50,000 waveforms from limitations of the computer processing power.

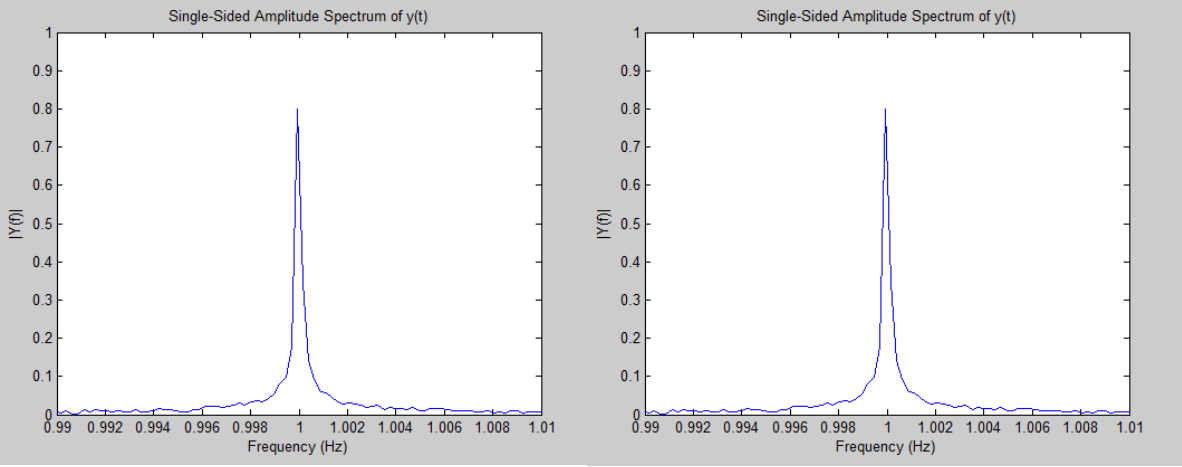


Figure 8: Plots of the FFT of the LVDT signal recorded over a 6 hour period running at a frequency of 1 Hz (left) and 2 Hz (right) while a total of six devices were operating. Samples consisted of 50,000 waveforms.

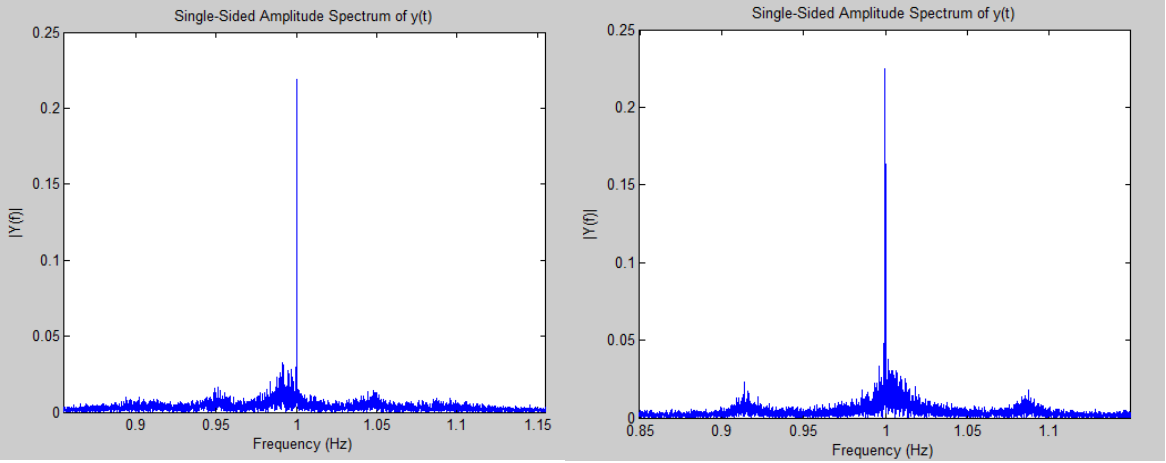


Figure 9: Plots of the fast Fourier transform of the LVDT signal recorded over a 6 hour period running at a frequency of 1 Hz under either a 10% Gaussian (left) or random (right) distribution. Samples consisted of 50,000 waveforms.

## 4.2 Characterization of the CHD Model

### 4.2.1 RNA Quantification of the F21 CHD Model

Phenotypic traits of the CHD model were determined by RNA expression extracted from digested and lysed heart samples using qRT-PCR. Fetal hearts from the nitrofen-induced CHD model and healthy groups were divided and analyzed in groups of CHD+, CHD- and healthy control sample. Four CHD+ samples, three CHD- samples and three control samples were analyzed. Several genes for the second sample group could not be analyzed due to sample limitations. Quantification was performed by probing for RNA related to contractile function (MYH6, MYH7, TNNT2, TNNI3, ACTN2, ATPA2), gap junction signaling (GJA1, CDH2) and markers of cardiac lineage (GATA4, GATA6, NKX2-5). Thresholds and Ct values for each gene was automatically designated by software provided with Mx3000P QPCR System. Based on assessment by Applied Biosystems and previous evaluations of matching amplification efficiency amongst probes used, $2^{-\Delta\Delta ct}$ was used for relative quantification of gene expression. Expression was normalized to GAPDH with healthy cardiomyocytes cultured in static conditions used as an untreated control population. Single outliner values were removed from triplicates if

remaining Ct values showed good correlation. Amplification past the designated threshold for all these genes was observed within 20-30 cycles with amplification plots following the expected exponential, linear and plateau pattern on a semi-log scale with tight clustering of amplification curves.

Samples for F21 time point were taken from multiple biological samples each consisting of a collection of hearts from a litter. ΔΔCt values were averaged and fold change was calculated to determine traits from each group that were statistically relevant (Figure 10). Individual sample data was is presented in the Appendix (Figure A1, A2, A3). Gene expression that displayed a two-fold shift was considered significant. The nitrofen-induced CHD+ group was observed to have significantly lower expression of MYH6 along with all gap junction and channel protein related genes compared to the control group. Other contractile proteins were observed to have slightly lower gene expression; however, these were not significant. In contrast, only RYR2 expression was significantly decreased in the CHD- group. Gene expression of TNNI, ACTN2, GATA4, GATA6 and NKX25 were significantly increased with slightly higher expression of TNNT2 and ATP2A2.

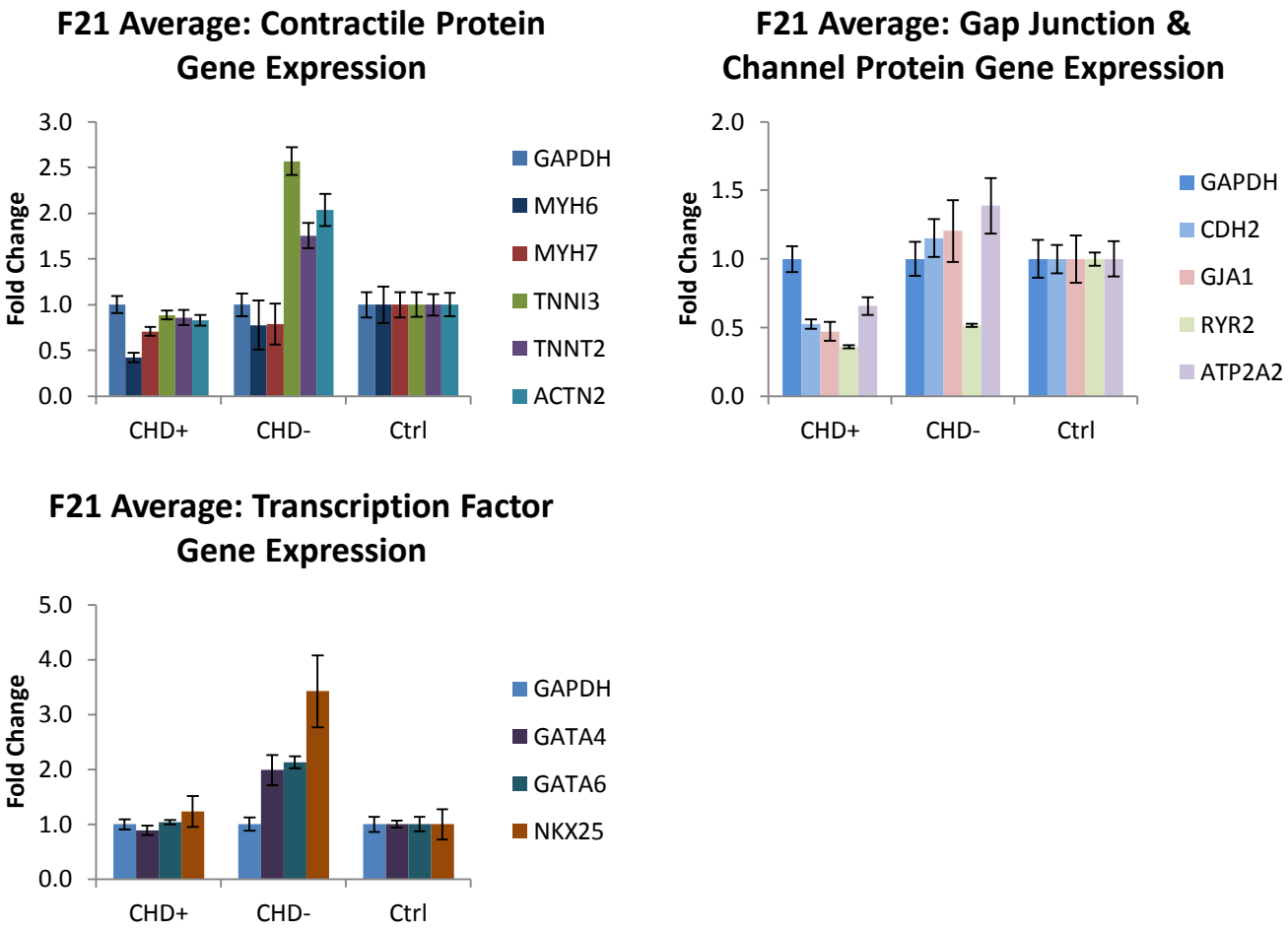


Figure 10: Plots of fold change in gene expression of contracile gap junction, channel and transcription factor proteins determined by qRT-PCR for F21 hearts. Averaged ΔΔCt was determined for four CHD+, three CHD- and three control biological samples.

### 4.2.2 RNA Quantification of F18 and E15 CHD Rat Model

To gain better understanding of development leading up to the characteristics of our observed CHD model, gene expression at time points F18 and E15 were also studied (Figure 11, 12). Samples at F18 were divided into CHD+, CHD- and control groups while only CHD+ and control samples were collected for E15 due to the difficulty differentiating development of a hernia at such an early developmental stage. Each set of sample data was taken from one biological sample. Experimental conditions and set-up matched those used for RNA quantification for the F21 time point.

The F18 CHD+ model displayed significant two-fold decreases in MYH6, TNNT2 and RYR2 with lesser shifts in TNNI3, ACTN2, and GATA4. A significant two-fold increase was determined for NKX25 with a lesser shift in MYH7. The CHD- model displayed similar patterns with additional significant decreases in CDH2 and ATP2A2 along with decreased expression of MYH7 and GATA6. NKX25 also showed increased expression, but to a lesser extent. Assessment of the E15 CHD+ model showed no significant shifts from the control group.

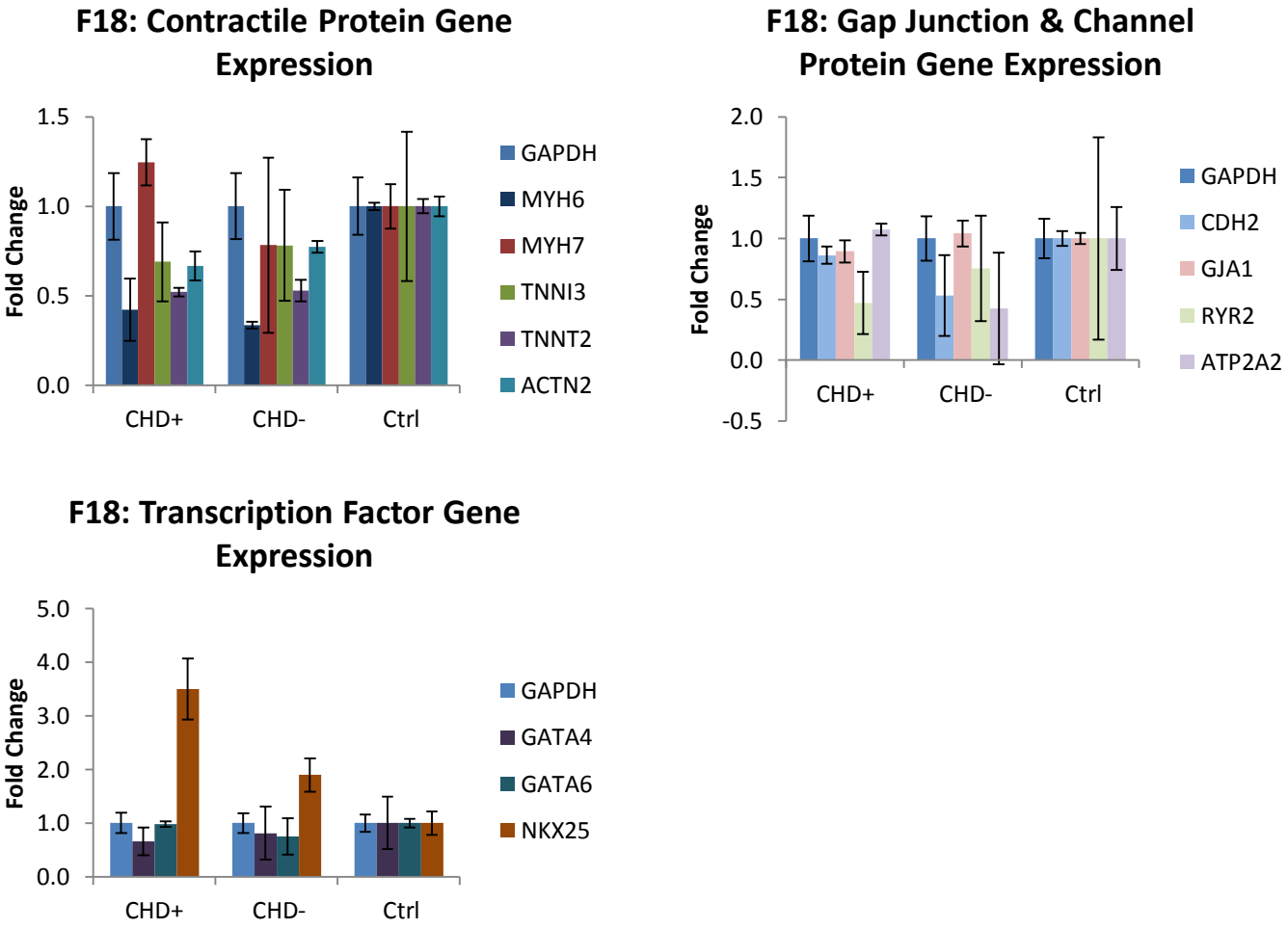


Figure 11: Plots of fold change in gene expression of contracile gap junction, channel and transcription factor proteins determined by qRT-PCR for F18 hearts. Sample consisted of a collection of fetal hearts isolated at F18 with 6 CHD+, 4 CHD- and 9 Ctrl hearts. RNA was isolated by silica column.

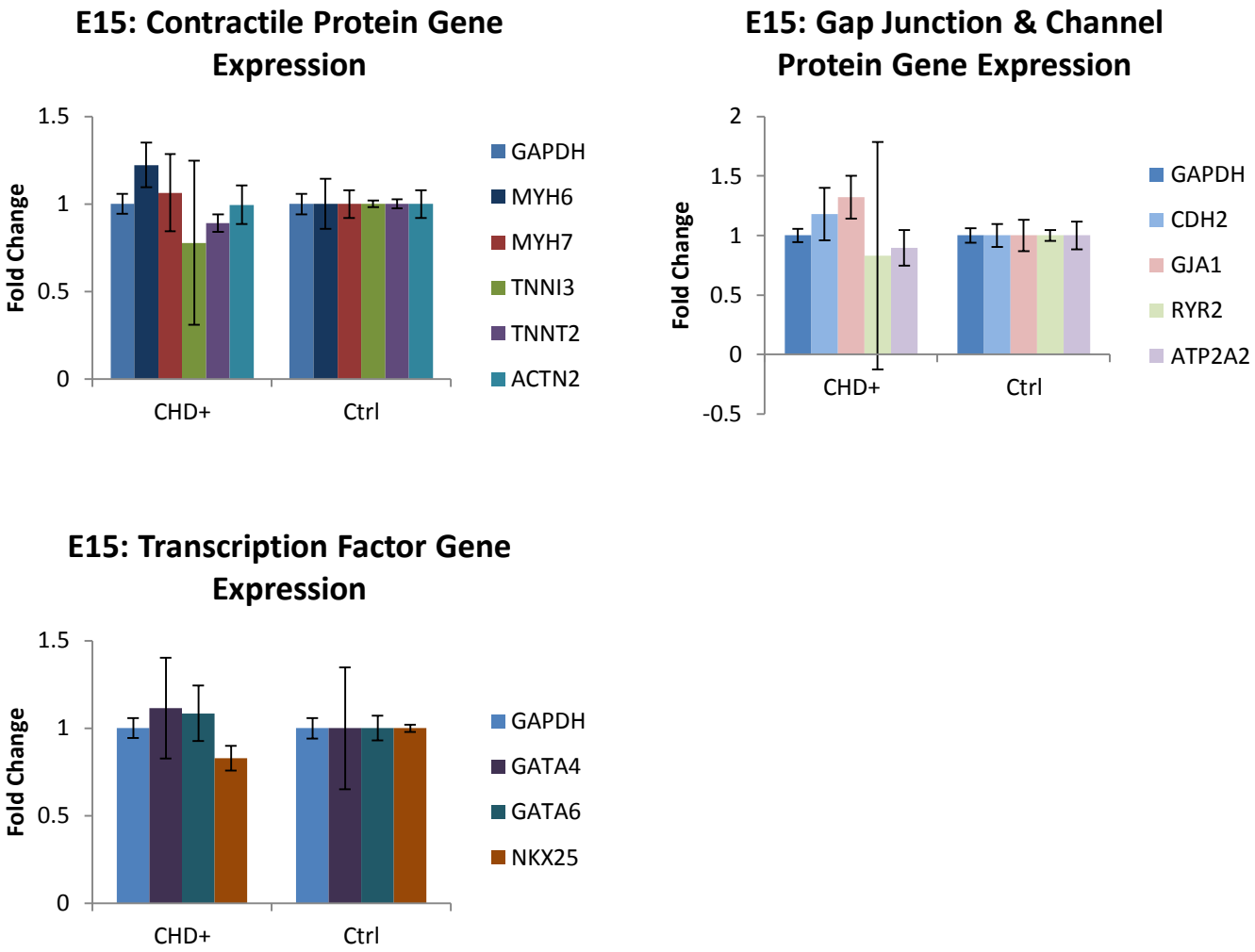


Figure 12: Plots of fold change in gene expression of contracile gap junction, channel and transcription factor proteins determined by qRT-PCR for E15 hearts. Sample consisted of a collection of fetal hearts isolated at F18 with 6 CHD+, 5 CHD- and 10 Ctrl hearts. RNA was isolated by TRIzol method.

### 4.2.3 Protein Quantification of the F21 and E15 CHD Model

As additional evaluation, protein content was analyzed by Western blot. Protein samples from F21 and E15 were successfully transferred and analyzed by antibody staining. Protein samples from F18 could not be quantified due to limited sample obtained for the control group. Additionally, only MYH-β, TnnT, N-cadherin, Cx43 and Gata4 were analyzed because several proteins could not be quantified due to lack of an observed signal when antibody assays were performed. Samples were normalized to β-actin which demonstrated a strong signal amongst

sample lanes. Although similar β-actin expression was desired between sample lanes, variations in pipetting, antibody binding and error in BCA determination led to observed differences in β-actin signal.

Due to difficulties with optimal antibody concentrations, only a limited amount of protein data could be acquired through Western blot quantification. Although the amount of protein quantified was limited, protein expression patterns for F21 were different from RNA expression patterns such as higher gap junction protein content. Additionally, E15 protein expression for CHD+ was much higher than the control which did not match observed RNA expression, thus indicating differences between RNA and protein expression.

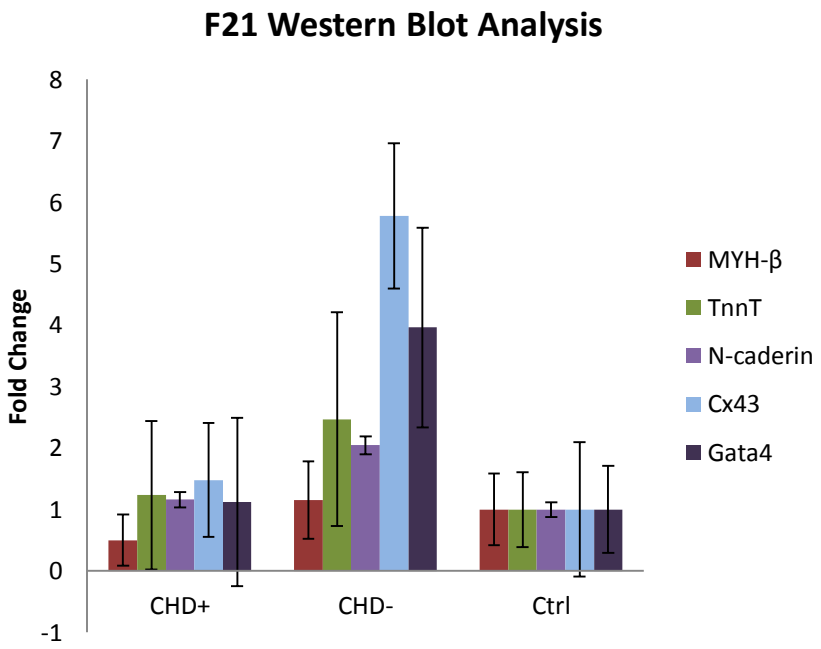

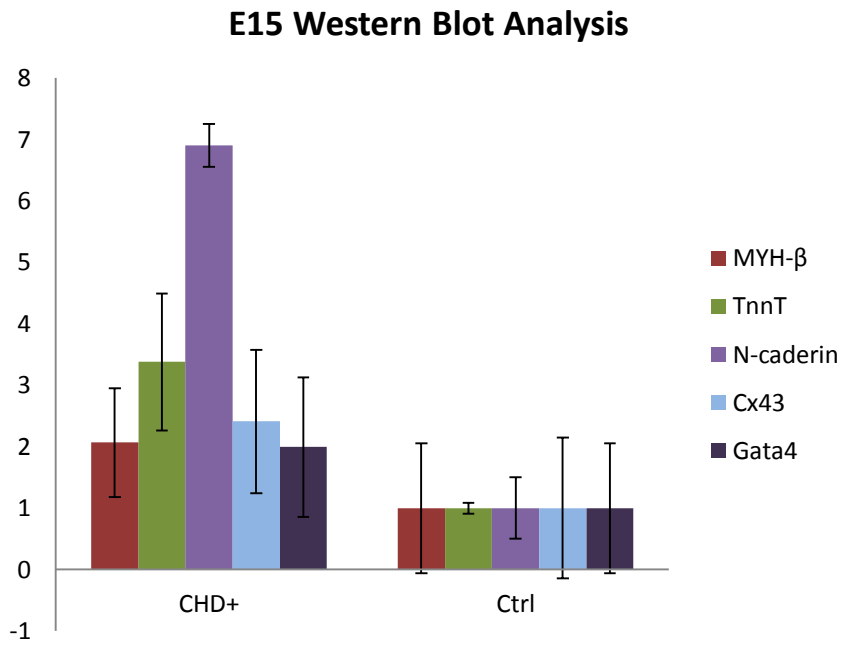


Figure 13: Plots of fold change in protein expression for contracile gap junction, channel and transcription factor proteins determined by Western blot and analzyed by ImageJ. Collection of F21 hearts were lysed together consisting of 5 CHD+, 4 CHD- and 5 Ctrl hearts. Collcetion of E15 hearts were lysed consisting of 6 CHD+ and 8 Ctrl hearts. Protein was isolated by cell lysis solution for E15 and TRIzol method for F21.

### 4.3 Effects of Mechanical Stimulation on Cardiac Cell Development

#### 4.3.1 RNA Quantification of Stretched Cardiac Cell Populations

Cardiac cells isolated from CHD+, CHD- and control fetal hearts were cultured on Pronectin BioFlex Culture Plates® under mechanical stimuli from the cell stretcher. Conditions for the mechanical stretch were dynamic environment based on the volumetric loading waveform of the left ventricle at 2% stretch with a constant, Gaussian and random frequency distribution. Additionally, a plate under a Gaussian amplitude distribution was cultured from 1.5 to 2.5% stretch. As a control, an additional plate was cultured under static conditions. These cells were planned to be cultured for two days statically to ensure good adherence followed by three days under mechanical stimulus. Good cell adherence and beating of myocytes was observed in the wells prior to loading onto the device. Unfortunately due to problems with cardiac cell retention

on culture plates under stimulated conditions, the experiment was terminated early after two days culture under mechanical stimulus. Cells that did maintain adherence were limited to CHD+ and healthy cell populations cultured statically and under variable mechanical strain following a Gaussian distribution from 1.5 to 2.5% stretch. Assessment for good sample quantity and quality were also limited to these two culture types which matched cell retention observations (Figure 13).

RNA quantification methods matched those used for characterization of the CHD model. Ct values were generally much higher than expected in the upper 20 to 40 range, however good correlation between triplicates was observed for several genes including GAPDH expression for normalization. Healthy myocytes grown statically was selected as the untreated control group. CHD+ cells cultured statically did show several shifts with tight standard deviation from the healthy control. These shifts were increased expression of MYH7, GJA1, RYR2 and GATA4 with TNNT2 and NKX25 showing significant decreased expression. For control cells cultured under mechanical stimulus TNNT2, ACTN2, CDH2, GJA1, RYR2 and GATA4 were significantly increased while NKX25 was significantly decreased. Finally, for the CHD+ population under mechanical stimulus all contractile proteins expect TNNT2, gap junction, channel and transcription factor proteins except for NKX25 were significantly increased.

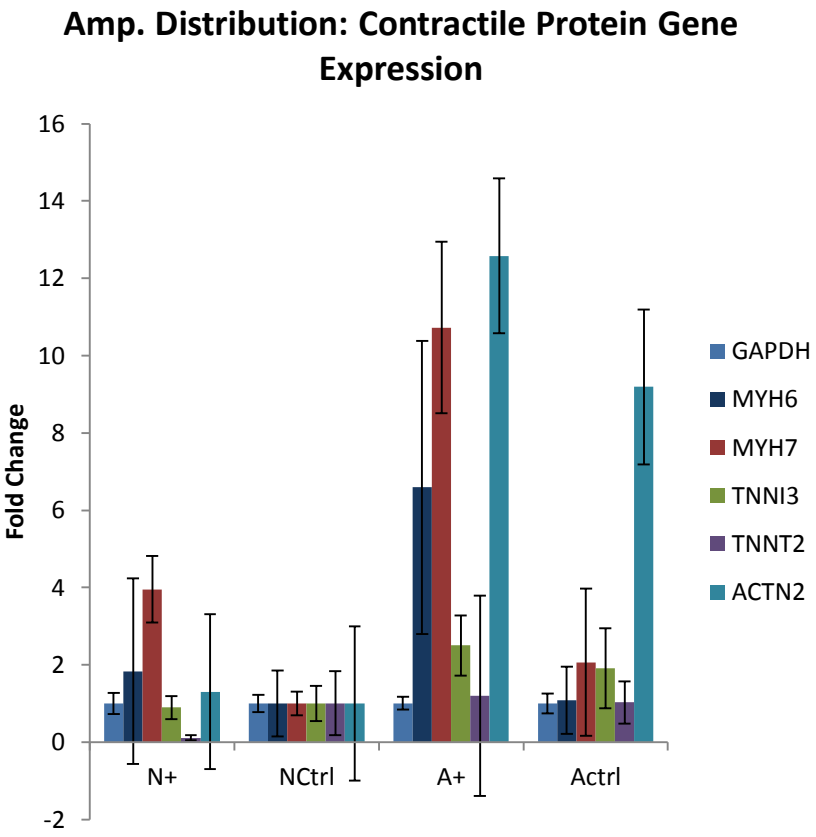
Amp. Distribution: Contractile Protein Gene Expression
Fold Change
16
14
12
10
8
6
4
2
0
-2
N+
NCtrl
A+
Actrl
GAPDH
MYH6
MYH7
TNNI3
TNNT2
ACTN2

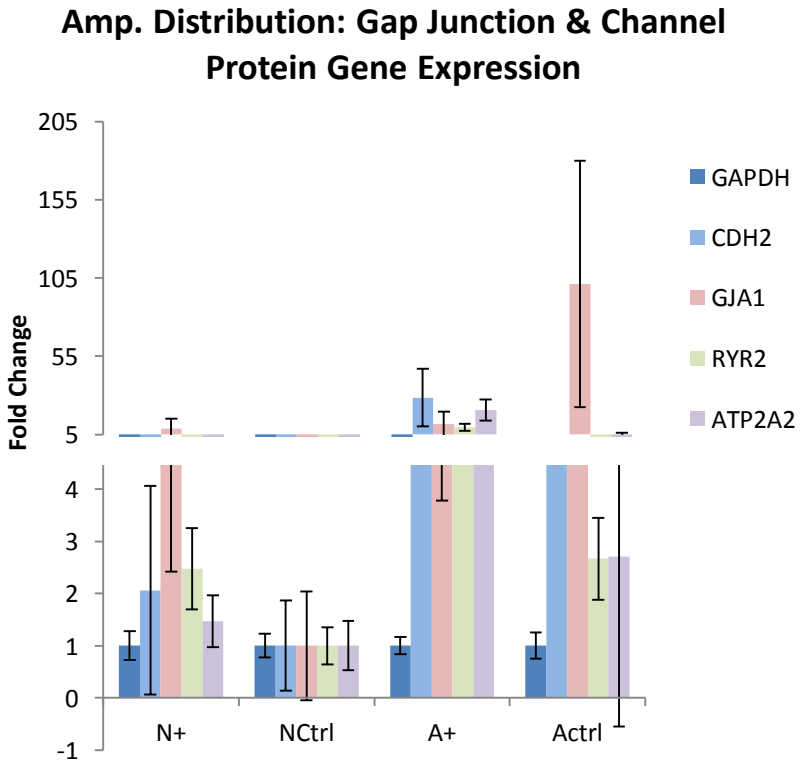
Amp. Distribution: Gap Junction & Channel Protein Gene Expression
Fold Change
205
155
105
55
5
4
3
2
1
0
-1
N+
NCtrl
A+
Actrl
GAPDH
CDH2
GJA1
RYR2
ATP2A2

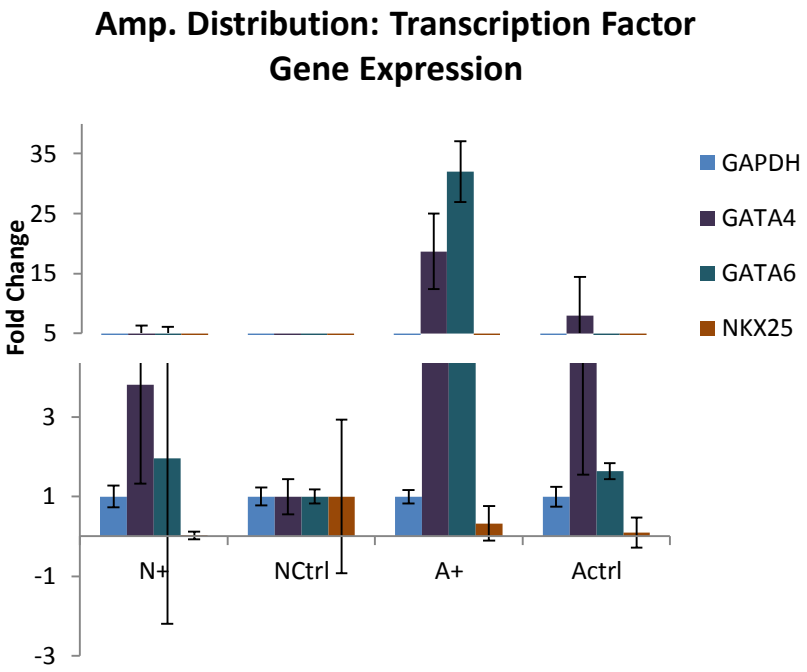


Figure 14: Plots of fold change in gene expression of contracile gap junction, channel and transcription factor proteins determined by qRT-PCR for statically cultured and mechanical stimulated fetal hearts. Each group had consisted of one sample cell culture population. RNA was isolated by TRIzol method.

### 4.4.2 Protein Quantification of Stretched Cells

Although protein sample was successfully isolated and Western blotting was performed on the sample, several complications limited the ability to analyze the sample such as lack of high molecular weight proteins observed on the blot and no signal was observed for β-actin to normalize results for other proteins.

## 5. Discussion

Our goal of this study was to analyze the role of the effects of varying mechanical environments on healthy and CHD cardiomyocyte development. We created and validated a model of the real-time dynamic stretching through cell culture on a silicone membrane while be stretched by a custom-built cell stretcher. A nitrofen-induced rat model of HLHS was also

created that was characterized for its phenotypic traits by RNA and protein quantification of biomarkers related to proper function and development of cardiomyocytes. Culture of cardiac cells form these groups under mechanical stimulation allowed us to investigate effects of mechanical cues on cardiomyocye development. By correlating changes in RNA and protein expression with the initial phenotypic conditions, the role of the mechanical environment on myocyte development was studied.

### 5.1 Generation and Validation of Mechanical Environment

Our custom-built cell stretcher device was designed to mimic the real-time dynamic mechanical stretching of the heart membrane by utilizing the fast activation and response time of a magnetic linear actuator. Development of our cell stretcher device and control system have allowed for stretching of a silicone culture membrane of up to 6% for six wells under arbitrary waveforms running at a rate 2 Hz under variable amplitude or frequency based on a set distribution. Considering our device was custom-built, it was important that we validated the characteristics of the device to properly assess whether we were creating our designated mechanical environment. Analysis of the membrane surface under mechanical stimulation demonstrated differences in the expected relationship between the plunger displacement and membrane stretch based on our conical frustum model. Actual percent stretch was observed to be both greater and following a more linear relationship compared to the exponential change of our membrane model. Considering that cell retention under mechanical stimulation has been a major limitation of our device for cardiac cell culture, this result indicated that culture conditions were harsher on the cell population than expected and could be lowered to hopefully improve observed cell retention. Possibility of other factors leading to loss of adherence have been

investigated, however cardiac cells have generally demonstrated very good adherence with pre-coated Pronectin silicone membrane under static conditions, but one to two days of mechanical stimulation has led to the majority of adhered cells lifting off the plate. Membrane stretch was determined to be relatively uniform over the plunger-membrane interface allowing for the possibility of accessing specific effects of different membrane stretches.

Analysis of the frequency output running multiple devices under constant frequency of 1 and 2 Hz by FFT demonstrated tight distribution around the designated frequency conveying our control of the rate of mechanical stimulation. Additionally, analysis of the output under a set frequency distribution did confirm a distributed output; however, shifts in center of the distribution and plot shape indicated differences from our designated parameters. These shifts were likely due to corrections made by the controller system to avoid issues with the system limitations such as microsecond rounding and response time of the device, thus actual distribution output was restricted. Furthermore, limitations to cell retention and computer processor speed have restricted our ability to culture cells at a rate mimicking the rat heart at 4 Hz which was previously achieved with simpler controller set-ups. Therefore, results of the validation indicated relatively good control of the mechanical environment created with possible improvements to the coding efficiency, system hardware and models of the environment allowing for improved accuracy of the designated mechanical environment.

Currently other systems such as the Flexcell 4000 cell stretch vacuum have been used to culture myocytes while being regularly stretch under similar culture conditions used for this study (Richard 2007, Komuro 1989). However, the selected frequency of 1 Hz and percent stretch up to 2.5% is not a limitation of our system. Our device has previously demonstrated output of highly defined waveforms at greater mechanical stretch up to 15% and frequencies up

to 4 Hz which is a limitation of the Flexcell 4000 system and would better match conditions of the native rat heart (Ace Animals, Inc 2008, Colombo 2008, Komuro 1990). Interestingly, the major limitation of our system for cell culture experiments was the commercial culture plates and problems maintaining cell retention while being mechanically stimulated. Thus besides improving our system's stretcher capabilities, improved cell adhesion to the silicone membrane or replacement of the commercial plates are needed to utilize the capabilities of our system.

### 5.2 Characterization of the CHD Model

To determine the initial condition of the cardiac cell population used in our study along with understanding the phenotypic traits related to the diseased condition, extensive characterization of the CHD rat model was performed. Phenotypic traits of the model were determined by RNA quantification to evaluate gene expression of biomarkers related to myocyte contractile function and development. The majority of the characterization was performed on samples at F21 with investigation of earlier time points at F18 and E15 for additional understanding of CHD development. Generally for qRT-PCR, two-fold and greater changes with tight standard deviations were considered significant shifts in gene expression due to lack of a known statistical method to determine significance amongst multiple biological samples.

Averaged shifts in gene expression from multiple samples of the F21 rat model showed shifts mainly related to MYH6, gap junction and channel proteins. These results indicated decreased myocyte function related to its contractile capability and myocyte connectivity. Additionally, studies have indicated that shifts in MYH-α, the protein product of MYH6, is related to cardiac immaturity and several disease rat models (Sengupta 2007). Although the shift from myosin heavy chain β to pre-dominantly α occurs through development to adulthood and

the rat heart consists mainly of the β isoform at this time point, early decreased expression of MYH6 could indicate restrictions to reaching cardiac maturity and decreased cardiac function (Lompre 1984). The detrimental effects of decreased MYH6 expression and MYH-α content is observed in humans which constituents only 25-35% of MYH RNA and 10% of the MYH protein content. Although these isoforms make up only a small portion of MYH RNA and protein, their amounts and expression are severely decreased during chronic heart failure, thus illustrating the detrimental effects of shifts to MYH isoforms (Lowes 1997, Nakao 1997, Miyata 2000, Reiser 2001).

Additionally, CHD- fetuses from the nitrofen model without an observed hernia demonstrated traits that were clearly distinct from CHD+ fetuses with a hernia present. Most genes were found to have expression either similar or greater than the control except for RYR2. One explanation for shifts in expression despite no hernia development was that the cardiac cell population was immature due to effects of nitrofen exposure. Thus the increased expression was observed due to cells still undergoing delayed development stages which were hindered in the CHD+ condition due to compression of the heart. This explanation was supported by the observed increases in transcription factors related to early cardiac differentiation and increased troponin expression which indicate an immature developing population (Hunkeler 1991). Additionally, lower expression for RYR2 indicated immature calcium handling in myocytes from both groups (Janowski 2010).

Evaluation of the individual traits of the CHD samples did demonstrate variability of the model. Sample 1 consisted of a larger collection of fetal hearts and RNA quantification demonstrated similar expression patterns between the CHD+ and CHD- groups. Later samples consisting of quantification from smaller heart collections demonstrated distinct patterns of

expression between the groups. Considering that these samples represent averaged expression from a collection of fetal hearts that were visually separated into CHD+ versus CHD-, unintentional mixing of the hearts phenotypically belonging to each group was more likely to occur in larger collections. One method to overcome this limitation for further characterization is RNA and protein isolation from individual rat hearts. Considering that large quantities of RNA and protein sample were retrieved from two heart samples, individual assessment of phenotypic traits could be performed to get a large set of biological samples and determine statistically relevant shifts.

Changes in gene expression at F18 and E15 were also studied to improve understanding of CHD development. Similar to the F21 time point, decreases in MYH6 and RYR2 were obsereved along with unique shifts in tropnonin T and I content and a spike in NKX25 expression. These shifts indicated cardiac immaturity compared to the control. Additionally, the majority of shifts in gene expression matched between the CHD+ and CHD- group, likely due to the larger collection of heart samples. E15 indicated that no significant shifts occurred which was possibly due to too short of a time for effects due to nitrofen and a distinct hernia to develop. Additionally, the time point selected could simply be a period that no significant shifts in gene expression are observed since shifts in GATA4 and GATA6 have been found at an earlier E13 time point (Takayasu 2008). However considering that no hernia was observed at the E15 time point, this observed downregulation could be due to nitrofen exposure. Therefore to improve our understanding of CHD development over the course of fetal stages, more time points and quantification of individual heart samples could be performed.

Western blotting was also performed to study the expression of the final protein product. Interestingly, several protein shifts at the F21 time point for the CHD+ condition were different

from the average shifts found from RNA expression such as normal gap junction protein expression. Protein content for the CHD- condition did relative match averaged patterns for the RNA expression. Additionally, protein expression for the E15 time point for the proteins assayed was all higher than the control which did not match with qRT-PCR results. One explanation for the differences observed was that too few biological samples were analyzed and certain shifts were sample specific. Another explanation was shifts in overall protein content due to changes in gene expression were delayed, thus protein quantification at neonatal stages were needed to find changes in gap junction and channel protein content. Considering that qRT-PCR results for the F18 stage indicated normal expression for CDH2 and Cx43, shifts in gene expression found at F21 could have occurred at that time point. Additionally, analysis by T-test gave P values greater than 0.05 indicating that the differences were not significant. However, cell lysis sample was taken from a single combined litter for the CHD+, CHD- and control condition compared to multiple samples analyzed by qRT-PCR, thus more protein analysis was needed to determine significant results. Thus to improve our analysis, more biological samples from various time points are required and by utilizing the TRIzol method, specific correlations between RNA and protein expression for individual biological samples can be made.

### 5.3 Effects of Mechanical Stimulation on Healthy and Diseased Myocyte Development

Due to limited cell retention and difficulty with retrieving enough quality RNA sample for analysis, results for cell culture experiments under mechanical stimulation was limited to CHD+ and control cell cultures under static and variable strain with a Gaussian distribution from 1.5 to 2.5% stretch. However, this study provided some understanding on the role of the mechanical environment. We found that gene expression in healthy cardiac populations cultured

in static and mechanically stimulated environments resulted in increased MYH6, MYH7, TNNI3, ACTN2, ACTN2, GJA1, RYR2, ATP2A2 and GATA4 with decreased NKX25. Based on the amount of genes with increased expression and large fold change observed, mechanical stimulation was found to greatly stimulate genes related to proper contractile function and myocyte activity. However, increased expression of MYH7 has been observed in failing adult mouse hearts (Harada 1999). However during early developmental stages, the β isoform is dominant, therefore, the increased expression MYH7 could simply be due to the early development stage of the cardiac cell population (Lompre 1984). Additionally increases in both MYH6 and MYH7were observed, thus increased expression of MYH7 coupled with increased MYH6 might not be a maladaptive response at this time point and instead be a physiological cellular response similar to hypertrophy (Iemitsu 2001).

We also found that several shifts in gene expression for CHD+ cells occurred simply due to culture on the flexible silicone membrane. Significant increases were observed for MYH7, GJA1, RYR2, GATA4 while significant decreased expression was observed for TNNT2 and NKX25. Lesser increased expression was observed for MYH6, CDH2, ATP2A2 and GATA6. Interestingly, expression of several of these genes was initially decreased based on our characterization of our CHD model; therefore, altered mechanical cues from the silicone membrane alone could have triggered increased expression of these functional proteins that previously inhibited by their native diseased environment.

Finally, we found that mechanical stimulation of CHD+ resulted in large increased expression of contractile proteins except TNNT2, gap junction, channel and transcription factor proteins assayed. Although increased expression for several of these genes was observed for the statically cultured CHD+ population, the fold change was much greater for the stimulated

population. Distinct from the CHD+ static population was increased expression of MYH6, ATP2A2 and GATA6. Considering that higher expression was found for the CHD+ stimulated population, mechanical cues from stimulation and the flexible membrane could have had synergetic effect leading to higher overall expression. Comparing the alterations in gene expression under these various conditions, it can be concluded that culture under mechanical stimulation mimicking the myocardial environment upregulated gene expression; however, whether myocyte function and maturation were improved requires further study.

## 6. Conclusion

The cell stretcher device allows for highly controlled dynamically stretched cell culture based on our evaluations of the membrane stretch, waveform generation and frequency output. Furthermore, our evaluations have also given better understanding to the environment generated and possible improvements that would improve the accuracy of our experimental set-up. As hypothesized, characterization of our CHD rat model for phenotypic traits determined by qRT-PCR indicated inhibited myocyte function and maturation. Culture of these cells under mechanical stimulation of cardiac cell populations greatly increased gene expression of proteins related to myocyte function and maturation. Comparison of the genes upregulated to the initial phenotypic traits of our CHD rat model indicated increased expression of many genes that were previously inhibited, thus suggesting significant alterations to the pathological phenotype that could lead to an improved phenotypic state. With improvements of cardiac cell adhesion to the flexible culture membrane, this study could be continued to determine how specific changes to the mechanical environment can be used to determine effects on cell development and proliferation. Furthermore, study on the effects of the mechanical environment could be used to

elucidate the general effects of mechanical stimulation on cell development. Ultimately, we were able to better understand the phenotypic development of HLHS and demonstrate the potentially significant influence mechanical stimulation has on myocyte development.

## 7. Future Direction

As the role of extracellular factors on cardiomyocyte development is better understood, the potential for development of novel methods of treatment by targeting these factors is expanded with possibility of restoration to a healthy phenotype. Therefore, continuation should be performed with improvements to culture, analysis and our system's capabilities. Improvements to culture should focus on improved cell retention and specific culture of the myocyte population. Expansion of analysis should focus on better protein quantification by Western blot and LC-MS/MS. Finally, improvements to our system's capability would expand on control and extracellular factors mimicked by our device.

Firstly, improvements to cell retention would allow us to determine the effects of specific alterations to the mechanical environment without issues with loss of sample. Additionally further alterations to the environment could be studied such as the effects of greater mechanical stretch mimicking the estimated percent stretch of the myocardial membrane at 15%. Improved cell retention would also allow for more immediate and long term studies. Immediate mechanical stimulation after several hours to a day of static culture would minimize alterations to the myocytes phenotype simply due to alterations of their adhered surface from their native environment. Based on the results, shifts in gene expression already occur simply due to culture on the flexible silicone membrane and long term static culture could already cause significant phenotypic changes before mechanical stimulation is applied. Long term studies culturing fetal

cardiac cells for several months could be used to study whether mechanical stimulation influences gene and protein expression observed during maturation to adulthood.

Secondly although qRT-PCR allows for precise and accurate measurement of a variety of cardiac biomarkers, various biological processes such as RNA processing and inhibition might influence the formation of the final protein product. Therefore, improved Western blot methods and LC-MS/MS could be used to quantify the functional protein product. Western blot analysis was mainly restricted due to issues with antibody optimization leading to quickly fading signals that were not measureable signal for the majority of biomarkers analyzed. For more rapid analysis, LC-MS/MS can be used to assess protein content of our mechanical stimulated populations.

Finally, control of the stretcher system could be improved by upgrades to hardware leading to improved computer processing power and NI-DAQ capabilities that allow for more specific creation of the desired mechanical environment. Alternatively, improvements to the system's capability to mimic the myocardial membrane environment could be made. One possibility includes adhesion of a PAAM or fibronectin gel to the membrane surface allowing control of the stiffness which has been demonstrated to undergo alterations in diseased states and influence maturation of myocytes (Jacot 2008, Jacot 2010). Another possibility could be the addition of electric stimulation to device's capabilities which would mimic the electrical impulses experienced by cardiac cells in their native environment. With improvement to the accuracy of our device and expansion of its capabilities to mimic the native environment, we can better isolate alterations in cellular response due to changes in their extracellular environment.

## 8. Appendix

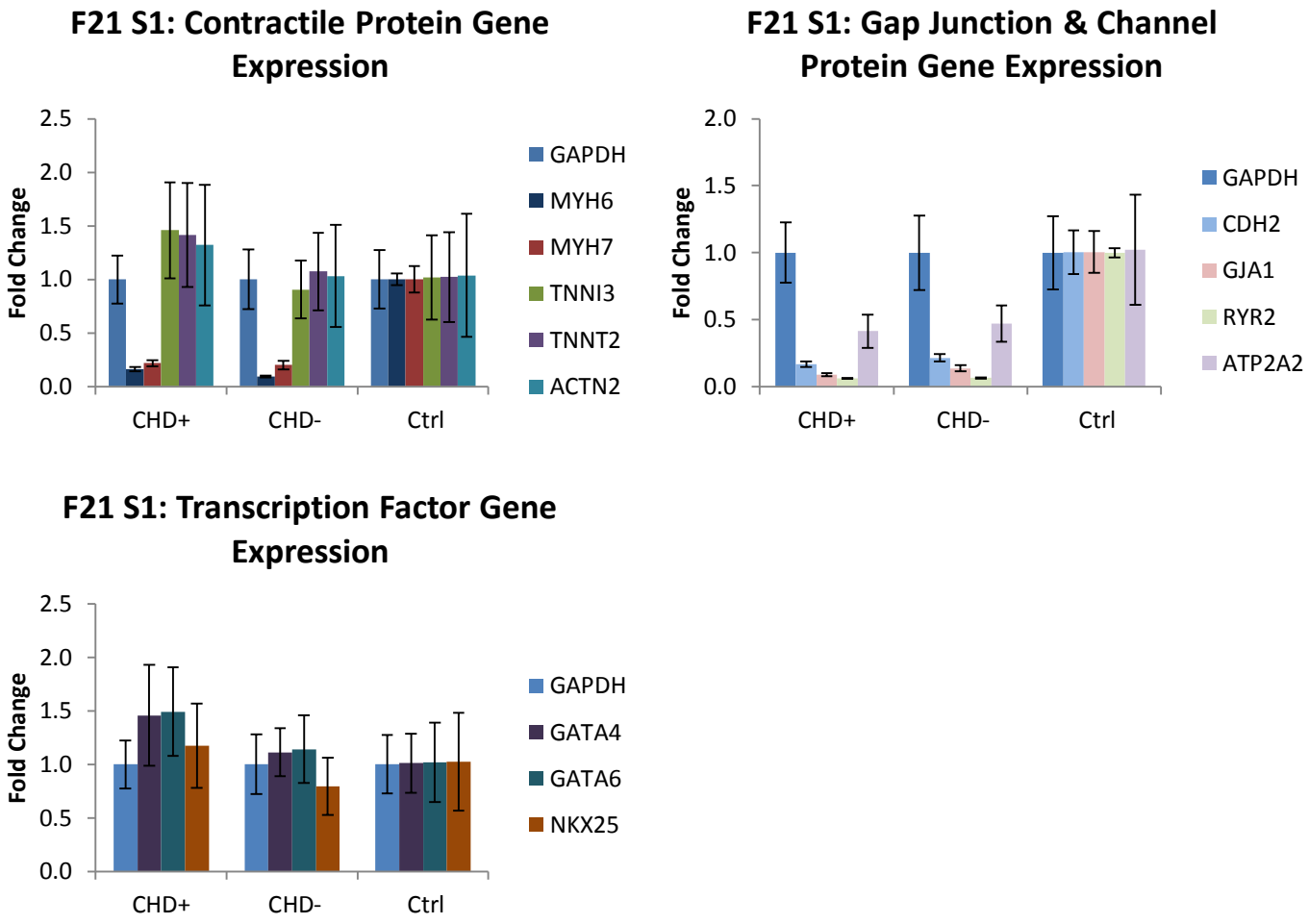


Figure A1: Plots of fold change in gene expression of contracile gap junction, channel and transcription factor proteins determined by qRT-PCR. Sample consisted of a collection of fetal hearts isolated at F21 with 7 CHD+, 6 CHD- and 12 Ctrl hearts. RNA was isolated by silica column.

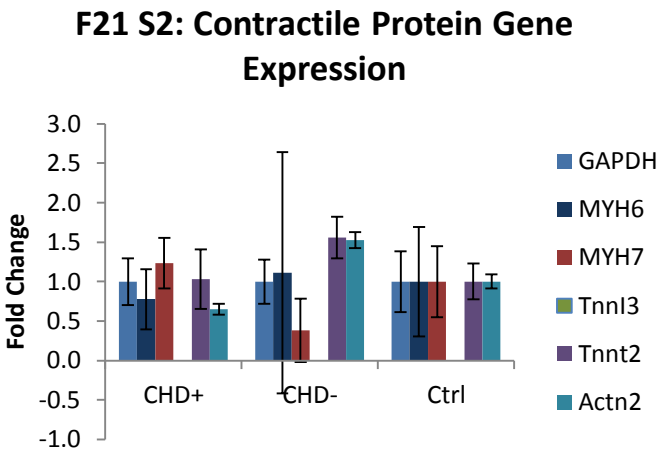


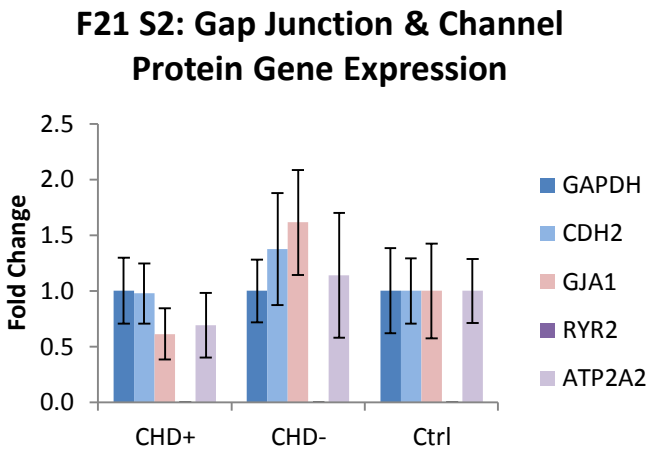


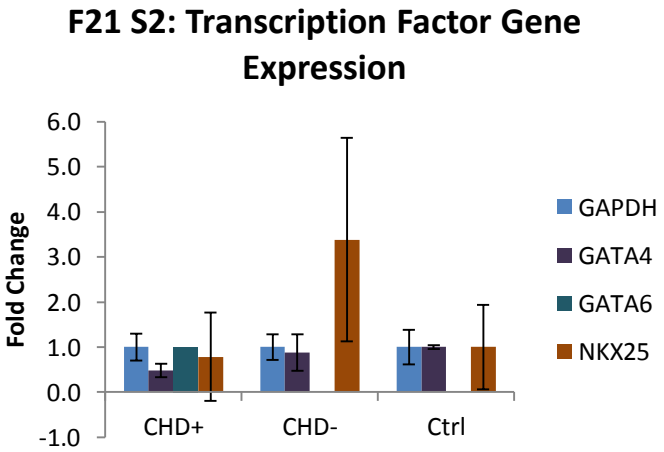


Figure A2: Plots of fold change in gene expression of contracile gap junction, channel and transcription factor proteins determined by qRT-PCR. Sample consisted of a collection of fetal hearts isolated at F21 with 5 CHD+, 4 CHD- and 5 Ctrl hearts. RNA was isolated by silica column.

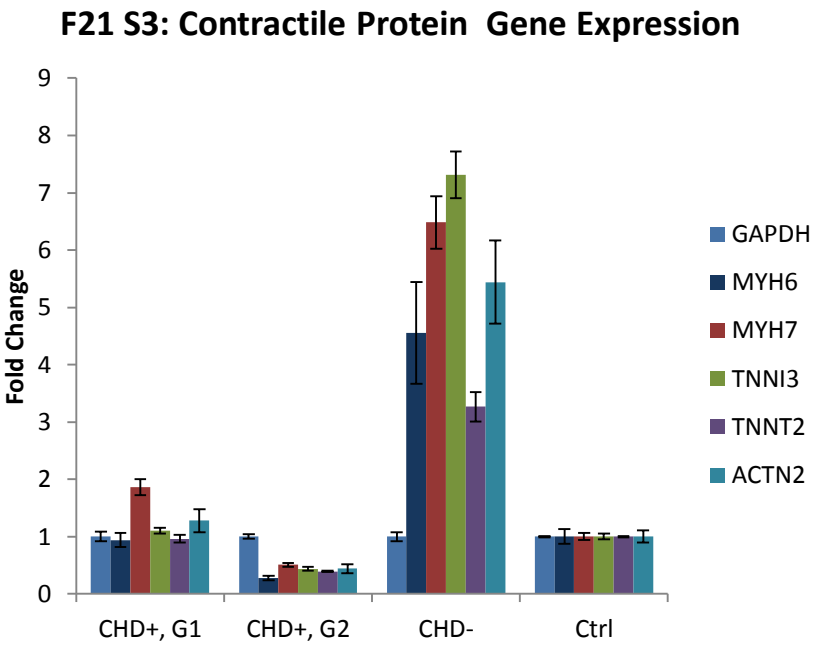
F21 S3: Contractile Protein Gene Expression
Fold Change
9
8
7
6
5
4
3
2
1
0
CHD+, G1
CHD+, G2
CHD-
Ctrl
GAPDH
MYH6
MYH7
TNNI3
TNNT2
ACTN2

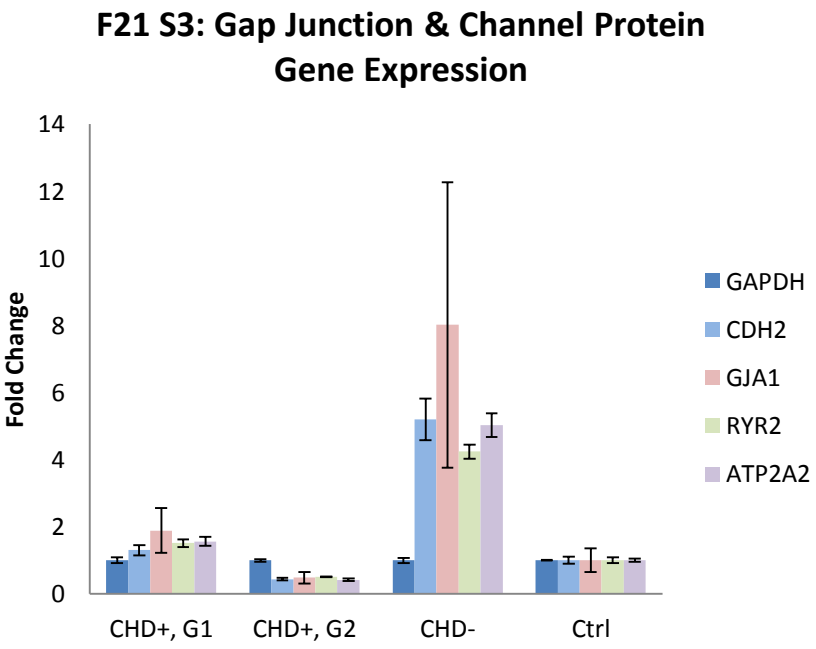
F21 S3: Gap Junction & Channel Protein Gene Expression
Fold Change
14
12
10
8
6
4
2
0
CHD+, G1
CHD+, G2
CHD-
Ctrl
GAPDH
CDH2
GJA1
RYR2
ATP2A2

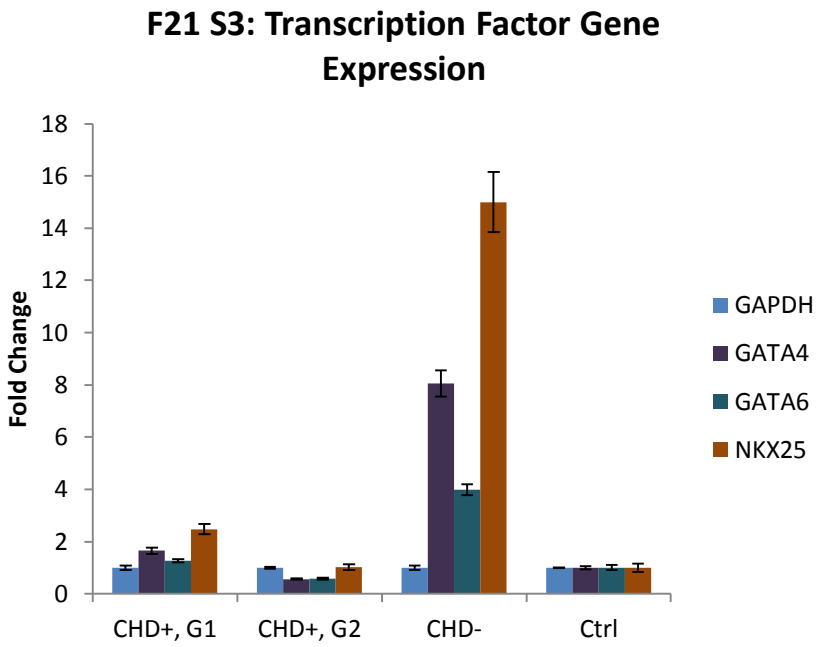


Figure A3: Plots of fold change in gene expression of contracile gap junction, channel and transcription factor proteins determined by qRT-PCR. Sample consisted of a collection of fetal hearts isolated at F21 with 2 CHD+ Group 1, 2 CHD+ Group 2, 2 CHD- and 2 Ctrl hearts. RNA was isolated by TRIzol method.

## 9. References


Ace Animals, Inc. Sprague Dawley. 2008. http://aceanimals.com/SpragueDawley.htm

A.D.A.M. Medical Encyclopedia. Hypoplastic left heart syndrome. PubMed Health. 2011.

American Heart Association (AHA). Heart disease and stroke statistics. 2011.

Black LD, 3rd, Meyers JD, Weinbaum JS, Shvelidze YA, Tranquillo RT. Cell-induced alignment augments twitch force in fibrin gel-based engineered myocardium via gap junction modification. Tissue engineering. 2009 Oct;15(10):3099-108.

Bupha-Intr Tepmanas, Holmes Jeffrey W., and Janssen Paul M. L. Induction of hypertrophy in vitro by mechanical loading in adult rabbit myocardium. AJP-Heart Circulation Physiology. 2007. 293: H3759-H3767.

Bround MJ, Asghari P, Wambolt RB, Bohunek L, Smits C, Philit M, Kieffer TJ, Lakatta EG, Boheler KR, Moore ED, Allard MF, Johnson JD. "Cardiac ryanodine receptors control heart rate and rhythmicity in adult mice".Cardiovasc. Res. 2012. 96(3): 372-380.

Chiu C, Bagnall RD, Ingles J, Yeates L et al. Mutations in Alpha-Actinin-2 Cause Hypertrophic Cardiomyopathy. J Am Coll Cardiol. 2010. 55(11): 1127-1135.

Colombo A, Cahill P A, Lally C. An analysis of the strain field in biaxial Flexcell membranes for different waveforms and frequencies. Engineering in Medicine. 2008. 222: 1235-1245.

Correia-Pinto Jorge, Baptista Maria J., Pedrosa Carla, Costa-Estevao Jose, Flake Alan W. and Leite-
Moreira Adelino F. Fetal Heart Development in the Nitrofen-Induced CDH Rat Model: The Role of Mechanical and Nonmechanical Factors. Journal of Pediatric Surgery. 2003. 38: 1444-1451.

deAlmedia Angela, McQuinn Tim and Sedmera David. Increased Ventricular Preload is Compensated by Myocyte Proliferation in Normal and Hypoplastic Fetal Chick Left Ventricle. Circulation. 2007. 100:1363-1370.

Fontan F and Baudet E. Surgical repair of tricuspid atresia. Thorax. 1971. 26(3): 240-248.

Fontes MS, van Veen TA, de Bakker JM and van Rijen HV. Functional consequences of abnormal Cx43 expression in the heart. Biochim Biophys Acta. 2012. 1818(8) 2020-2029.

Frank D, Kuhn C, Katus HA and Frey N. The sarcomeric Z-disc: a nodal point in signaling and disease. J Mol Med. 2006. 84: 446-468.

Fruitman Deborah S. Hypoplastic left heart syndrome: Paediatrics & Child Health. Prognosis and management options. 2000. 5(4): 219-225.

Gambetta K, Al-Ahdab MK, Ilbawi MN, Hassaniya N and Gupta M. Transcription repression and blocks in cell cycle progression in hypoplastic left heart syndrome. AJP-Heart. 2008. 294(5): H2268-H2275.

Goldberg Caren S. and Gomez Carlen A. Hypoplastic left heart syndrome: new developments and current controversies. Seminars in Neonatology. 2003. 8:451-468.

Guarino N., Shima H. and Puri P. The hypoplastic heart in congenital diaphragmatic hernia: reduced expression of basic fibroblast growth factor and platelet-derived growth factor. Pediatr Surg Int. 2000. 16: 243-246.

Hall JE. and Guyton AC. Textbook of Medical Physiology. 12e. Philadelphia, Pensylvania. Saunders/Elsevier. 2011.

Harada K, Sugaya T, Murakami K, Yazaki Y, Komuro I. Angiotensin II type 1A receptor knockout mice display less left ventricular remodeling and improved survival after myocardial infarction. Circulation. 1999. 100: 2093-2099.

Hunkeler NM, Kullman J and Murphy AM. Troponin I isoform expression in human heart. Circ Res. 1991. 69:1409-1414.

Iemitsu M, Miyauchi T, Maeda S, Sakai S, Kobayashi T, Fujii N, Miyazaki H, Matsuda M and Yamaguchi I. Physiological and pathological cardiac hypertrophy induce different molecular phenotypes in the rat. AJP Regu Physiol. 2011. 281(6): R2029-R2036.

Jacot JG, Martin JC, Hunt DL. Mechanobiology of cardiomyocyte development. J Biomech. 2010; 43:93-8.

Jacot JG, McCulloch AD, Omens JH. Substrate stiffness affects the functional maturation of neonatal rat ventricular myocytes. Biophys J. 2008. 95: 3479- 87.

Jalali Ali and Nataraj C. A Cycle-Averaged Model of Hypoplastic Left Heart Syndrome. 33rd Annual International Conference of the IEEE EMBS. 2011. 190-194.

Janowski E, Berrios M, Cleemann L, Morad M. Developmental aspects of cardiac $Ca^{2+}$ signaling: interplay between RyR- and $IP_3$ R-gated $Ca^{2+}$ stores. Am J Physiol Heart Circ Physiol. 2010. 298(6): H1939 - 50.

Jenkins Kathy J, Correa Adolfo, Feinstein Jeffrey A., Botto Lorenzoo, Britt Amy E., and et. al. Noninherited Risk Factors and Congenital Cardiovascular Defects: Current Knowledge. Circulation. 2007. 115: 2995-3014.

Kawashima Y, Kitamura S, Matsuda H, Shimazaki Y, Nakano S, Hirose H. Total cavopulmonary shunt operation in complex cardiac anomalies: A new operation. J. Thorac. Cardiovasc. Surg.1984. 87(1): 74–81.

Komuro I, Kaida T, Shibazaki Y, Kurabayashi M, Katoh Y, Hoh E, Takaku F and Yazaki Y. Stretching Cardiac Myocytes Stimulates Protooncogene Expression. The Journal of Biological Chemistry. 1990. 265(7): 3595-3598.

Krenz M and Robbins J. Impact of beta-myosin heavy chain expression on cardiac function during stress. J Am Coll Cardiol. 2004. 44(12): 2390-2397.

Kreutzer G, Galíndez E, Bono H, De Palma C and Laura JP. An operation for the correction fo tricuspid atresia. J Thorac Cardiovasc Surg. 1973. 66(4): 613-621.

Kushnir A and Marks AR. The ryanodine receptor in cardiac physiology and disease. Adv Pharmacol. 2010. 59: 1-30.

Larsen L. U., Petersen O. B., Norrild K., Sorensen K., Uldbjerg N. and Sloth E. Strain rate derived from color Doppler myocardial imaging for assessment of fetal cardiac function. Ultrasound Obstet Gynecol. 2006. 27: 210-213.

Latal B, Helfricht S, Fischer J, Bauersfeld U, Landolt M. Psycho-logical adjustment and quality of life in children and adolescents following open-heart surgery for congenital heart disease: a systematic review. BMC Pediatr 2009;9:6.

Loffredo Crhistopher A. Epidemiology of Cardiovascular Malformations: Prevalence and Risk Factors. American Journal of Medical Genetics. 2000. 97:319-325.

Lompre AM, Mercadier JJ & Schwartz K. Changes in gene expression during cardiac growth. Int Rev Cytol. 1991. 124: 137–186.

Lompre AM, Nadal-GinardB&Mahdavi V. Expression of the cardiac alpha- and beta-myosin heavy chain genes is developmentally and hormonally regulated. J Biol Chem. 1984. 259: 6437–6446.

Ludman P, Foale R, Alexander N and Nihoyannopoulos P. Cross sectional echocardiographic identification of hypoplastic left heart syndrome and differentiation from other causes of right ventricular overload. Br Heart J. 1990. 63(6): 355-361.

Miyata S, Minobe W, Bristow MR & Leinwand LA (2000). Myosin heavy chain isoform expression in the failing and nonfailing human heart. Circ Res. 2000. 86: 386–390.

Nakao K, Minobe W, Roden R, Bristow MR & Leinwand LA. Myosin heavy chain expression in human heart failure. JClin Invest. 1997. 100: 2362–2370.

Norwood WI, Kirklin JK, Sanders SP. Hypoplastic left heart syndrome: experience with palliative surgery. Am J Cardiol. 1980. 45: 87– 91

Periasamy M and Kalyanasundaram A. SERCA pump isoforms: their role in calcium transport and disease. Muscle Nerve. 2007. 35(4): 430-442.

Reiser PJ, Portman MA, Ning XH & Moravec CS. Human cardiac myosin heavy chain isoforms in fetal and failing adult atria and ventricles.Am J Physiol Heart Circ Physiol. 2001. 280: H1814–H1820.

Sano S, Ishino K, Kawada M, et al. Right ventricle-pulmonary artery shunt in first-stage palliation of hypoplastic left heart syndrome. J Thorac Cardiovasc Surg. 2003. 126: 504–509.

Sedmera David, Hu Norman, Weiss Karen M., Keller Bradley B., Denslow Stewart and Thompson Robert P. Cellular Changes in Experimental Left Heart Hypoplasia. The Anatomical Record. 2002. 267: 137-145.

Sengupta PP, Krishnamoorthy VK, Korinek J, Narula J, Vannan MA, Lester SJ, et al. Left ventricular form and function revisited: applied translational science to cardiovascular ultrasound imaging. J Am Soc Echocardiogr. 2007; 20(5):539- 51.

Soler AP and Knudsen KA. N-cadherin involvement in cardiac myocyte interaction and myofibrillogenesis. Dev Biol. 1994. 162(1): 9-17.

Takayasu Hajime, Hideaki Sato, Sugimoto Kaoru and Puri Prem. Downregulation of GATA4

and GATA6 in the heart of rats with nitrofen-induced diaphragmatic hernia. Elsevier. 2008. 43: 362-366.

Tanindi A and Cemri M. Troponin elevation in conditions other than acute coronary syndromes. Vasc Health Risk Manag. 2011. 7: 597-603.

Tobita Kimimasa, Schroder Elizabeth A., Tinney Joseph P., Garrison Jason B. and Keller Bradley B. Regional passive ventricular stress-strain relations during development of altered loads in chick embryo. Am J Physiol. Heart Circ. Physiol. 2002. 282: H2386-H2396.

Vink MJ, Suadicani SO, Vieira DM, Urban-Maldonado M, Gao Y, Fishman GI and Spray DC. Alterations of intercellular communication in neonatal cardiac mypcytes from connexin43 null mice. Cardiovasc Res. 2004. 62(2): 397-406.

Vogel M., McElhinney D.B., Marcus E., Morash D., Jennings R. W. and Tworetzky W. Significance and outcome of left heart hypoplasic in fetal congenital diaphragmatic hernia. Ultrasound Obstet Gynecol. 2010. 35: 310-317.

Yano M, Yamamoto T, Ikemoto N and Matsuzaki M. Abnormal ryanodine receptor function in heart failure. Elsevier: Pharmacology & Therapeutics. 2005. 107: 377-391.